DESIGN AND SYNTHESIS OF FLUORESCEIN BASED GOLD ION SENSORS

A Thesis Submitted to
the Graduate School of Engineering and Sciences of
İzmir Institute of Technology
in Partial Fulfillment of the Requirements for the Degree of

MASTER OF SCIENCE

in Chemistry

By
Ceyla ÇETİNTAŞ

July 2016
İZMİR

We approve the thesis of **Ceyla ÇETİNTAŞ**

Examining Committee Members:

Assoc. Prof. Dr. Mustafa EMRULLAHOĞLU
Department of Chemistry, İzmir Institute of Technology

Asst. Prof. Dr. Yaşar AKDOĞAN

Department of Materials Science and Engineering, İzmir Institute of Technology

Asst. Prof. Dr. Tuna SUBAŞI
Department of Food Engineering, Ahi Evran University

21 July 2016

Assoc. Prof. Dr. Mustafa EMRULLAHOĞLU
Supervisor, Department of Chemistry,
İzmir Institute of Technology

Prof. Dr. Ahmet Emin EROĞLU

Head of the Department of Chemistry

Prof. Dr. Bilge KARAÇALI

Dean of the Graduate School of Engineering and Science

ACKNOWLEDGEMENTS

Foremost, I would like to express my gratitude and admiration to my advisor Assoc. Prof. Dr. Mustafa Emrullahoğlu, who gave me opportunities, support, encouragement, patience and understanding. It is my great fortune to join Emrullahoğlu research group, and explore the most attractive field in chemistry under his guidance.

I would also like to thank the members of the research group especially Erman Karakuş, Muhammed Üçüncü, İklima Kırpat, Hüseyin Zeybek and Ceren Cantürk for your willingness to always help me.

I am also very grateful to my committee members, Asst. Prof. Dr. Yaşar Akdoğan and Asst. Porf. Dr. Tuna Subaşı. I really appreciate their precious time and continual support.

I would like to thank the TUBITAK (113Z601) and IZTECH for supporting me during this project.

Finally, I want to thank my family for providing me all the moral support whenever I needed it the most. My parents, İnci Çetintaş and Salih Çetintaş, and all my friends for providing love and support everytime that I got desperate. Last but not the least; I would like to thank my love, Doğukan Akın for loving me unconditionally and making me have faith in me.

ABSTRACT

DESIGN AND SYNTHESIS OF FLUORESCEIN BASED GOLD ION SENSORS

Gold has been a part of people's lives for ages and is used as money, goods and jewellery. In recent years, gold has played a key role in chemistry, medicine and biology. Since the 1970s, gold has been extensively used as a catalyst in several chemical transformations. Due to its high biocompatibility, functionalized gold nanoparticles have been extensively employed as drug and gene delivery systems, biosensors and bio-imaging materials. However, gold complexes can become toxic to the human body by interacting with biomolecules such as DNA and enzymes. Therefore, detection of trace amounts of gold species is an important issue and can be achieved via spectroscopic methods such as atomic absorption spectroscopy, atomic emission spectroscopy and inductively coupled plasma spectrometry. However, these analytical methods require complicated sample preparation steps and sophisticated instrumentation. In contrast to these extremely expensive and time-consuming methods, fluorogenic or chromogenic methods, which provide high analyte sensitivity and selectivity, can serve as good alternatives for detecting gold species.

To develop new probes for the detection of Au^{3+} ions, we focused on the design of new fluorescein-based probes that are soluble in aqueous media. We aimed to investigate the in vivo activity of these fluorescent probes. In the proposed detection system, gold ions are expected to mediate a chemical reaction through coordination to an alkyne moiety that results in a ring opening reaction to yield a highly fluorescent derivative.

ÖZET

FLORESEİN BAZLI ALTIN İYON SENSÖRLERİNİN TASARIMI ve SENTEZİ

Altın, ilk uygarlıkların sarı parlayan külçeler halinde keşfettiği ilk metaldir. Altın yüzyıllar boyunca insanların hayatında para, eşya ve takı gibi birçok farklı alanda kullanılmıştır. Son yıllarda altın türevleri kimya, tıp ve biyoloji alanlarında önemli bir rol oynamıştır. 1970'li yıllardan günümüze altın türevleri birçok kimyasal reaksiyonda katalizör olarak kullanılmıştır. Romatoid artrit, astım, tüberküloz, sıtma, kanser, HIV ve beyin lezyonları gibi çeşitli hastalıkların tedavisinde altın bazlı ilaçlar kullanılmaktadır. Altın nanoparçacıkları, biyolojik sistemlere uyumlu olması sebebiyle, ilaç ve gen taşıma amaçlı ve biyo-görüntüleme malzemeleri olarak kullanılmaktadırlar. Fakat altın kompleksleri DNA ve enzimler gibi biyo-moleküllerle kuvvetli etkileşimler yaparak insan vücudu için toksik olabilir. Bu sebeplerden dolayı, altın türlerinin eser miktarlarının tayini oldukça önemlidir. Atomik absorpsiyon ve atomik emisyon spektroskopisi, indüktif eşleşmiş plazma spektrometresi gibi spektroskopik yöntemler kullanılarak eser miktarda altın tayini yapılabilmektedir. Fakat bu yöntemler için karmaşık örnek hazırlama aşamaları ve sofistike cihazlar gerekmektedir. Oldukça pahalı ve zaman alıcı yöntemlerin yanı sıra, yüksek analit duyarlılığı ve seçiciliği olan, daha kolay örnek hazırlama ve daha basit cihazlar gerektiren florojenik ve kromojenik yöntemler ile eser miktarda altın tayini yapmak iyi bir alternatif olabilir.

Altın iyonlarının tayini için "Fluorescein" yapısında suda çözünür yeni kemosensörler tasarlamayı ve bu sensörlerin hücre ortamındaki aktifliğini belirlemeyi amaçlanmıştır. Bu çalışmada altın iyonunun alkinofilik özelliğinden ve floresein yapısının kendisine özgü olarak gerçekleştirdiği halka açılma reaksiyonundan faydalanılarak etkin bir sistem geliştirmek amaçlanmıştır. Böyle bir sistemde, ortamda bulunan altın iyonları kemosensörün üzerindeki alkin yapısıyla etkileşerek yeni bir yapı oluşturur ve halka açılma tepkimesi sonucunda bu bileşik floresan ışıma yapar.

TABLE OF CONTENTS

APPENDICES

LIST OF FIGURES

Figure **Page**

LIST OF ABBREVIATIONS

BODIPY	4, 4-difluoro-4-bora-3a, 4a-diaza-s-indacene
DCM	Dichloromethane
RT	Room Temperature
EtOH	Ethanol
NMR	Nuclear Magnetic Resonance
PBS	Phosphate buffered saline

CHAPTER 1

INTRODUCTION

1.1. An Overview

Gold, a unique metal, is widely disseminated in nature. Because of its useful physical and chemical properties, gold is extensively used in selective oxidation and photo-physical applications and as a catalyst; moreover, gold nanoparticles are used in diagnostics and detection.

The valence electrons in a gold atom occupy a 6s orbital and 5d orbitals; this electron configuration makes gold a strong π-bond acceptor. Gold ions are alkynophilic because of their strong Lewis acid character. Moreover, they can reflect infrared light, visible light and radio waves; therefore, they can be used in coatings for planes and satellites. In addition, gold exhibits anti-inflammatory properties and is widely used in the treatment of various diseases, including tuberculosis and arthritis. Gold-based drugs are used in the treatment of several diseases, including asthma, rheumatic arthritis, cancer, tuberculosis, malaria, HIV and brain lesions (Vasimalai et al., 2014).

However, gold ions can damage living organisms. The gold ion can easily bind to biomolecules and can cause gold toxicity, which damages the liver, kidneys and nervous system.

Therefore, it is important to detect gold ions because of their detrimental effects on the human body. There are several sensitive detection methods, including inductively coupled plasma optical-emission spectroscopy (ICP-OES), inductively coupled plasma atomic-emission spectroscopy (ICP-AES), inductively coupled plasma mass spectroscopy (ICP-MS) and anodic stripping voltammetry (Cao et al., 2011). However, none of these methods involve simple preparation and usage. A fluorescence-sensing method is highly desirable for easily obtaining accurate evidence. In addition, fluorophore cores can be adjusted according to their photophysical properties.

1.2. Fluorescein as a Fluorophore

In the past few decades, considerable effort has been put in the development of selective sensors with high capacity. These sensors, because of their useful properties, have been extensively used for the detection of trace metals. The design of organic molecules that can act as fluorophores is important for synthesis probes; these molecules must have selectivity and sensitivity. Different types of organic molecules have been used in fluorometric studies, including BODIPY, rhodamine and fluorescein. In this study, fluorescein was utilized as a fluorophore because of its individual performance.

Fluorescein, a classic fluorophore, was first synthesized by Adolf von Baeyer in 1871. This dark orange-red dye is obtained via a Friedel–Crafts reaction using a 1:2 ratio of phthalic anhydride to resorcinol in the presence of zinc chloride.

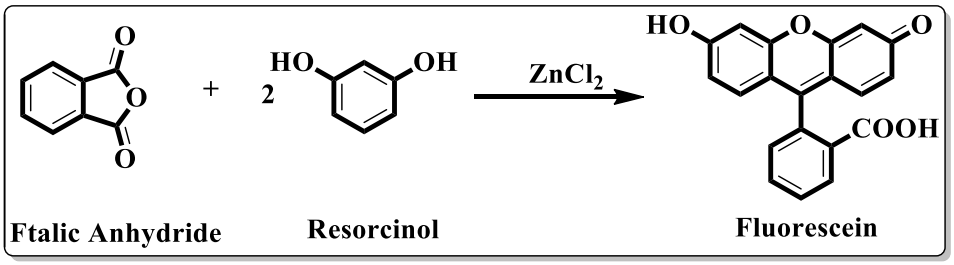

Figure1.1. Synthesis of fluorescein
(Source: Sun et al., 1997)

Fluorescein dyes have excellent properties of high absorption coefficient, high quantum yield, good photostability and long emission wavelength due to their xanthene scaffolds (Quimica et al., 2007).

In aqueous solutions, fluorescein can exist in cationic, anionic, neutral and di-anionic forms; this makes it pH-dependent for absorption and fluorescence activities. Fluorescein is cationic in acidic solutions. It is neutral at a pH of 2–4; at pH levels above 4 and below 6.4, fluorescein exists as a mono-anion. When its pH value reaches 6.4, fluorescein exists in its di-anionic form. Fluorescein exhibits its greatest fluorescent properties at a pH greater than 6.5; therefore, it requires a basic environment to perform optimally.

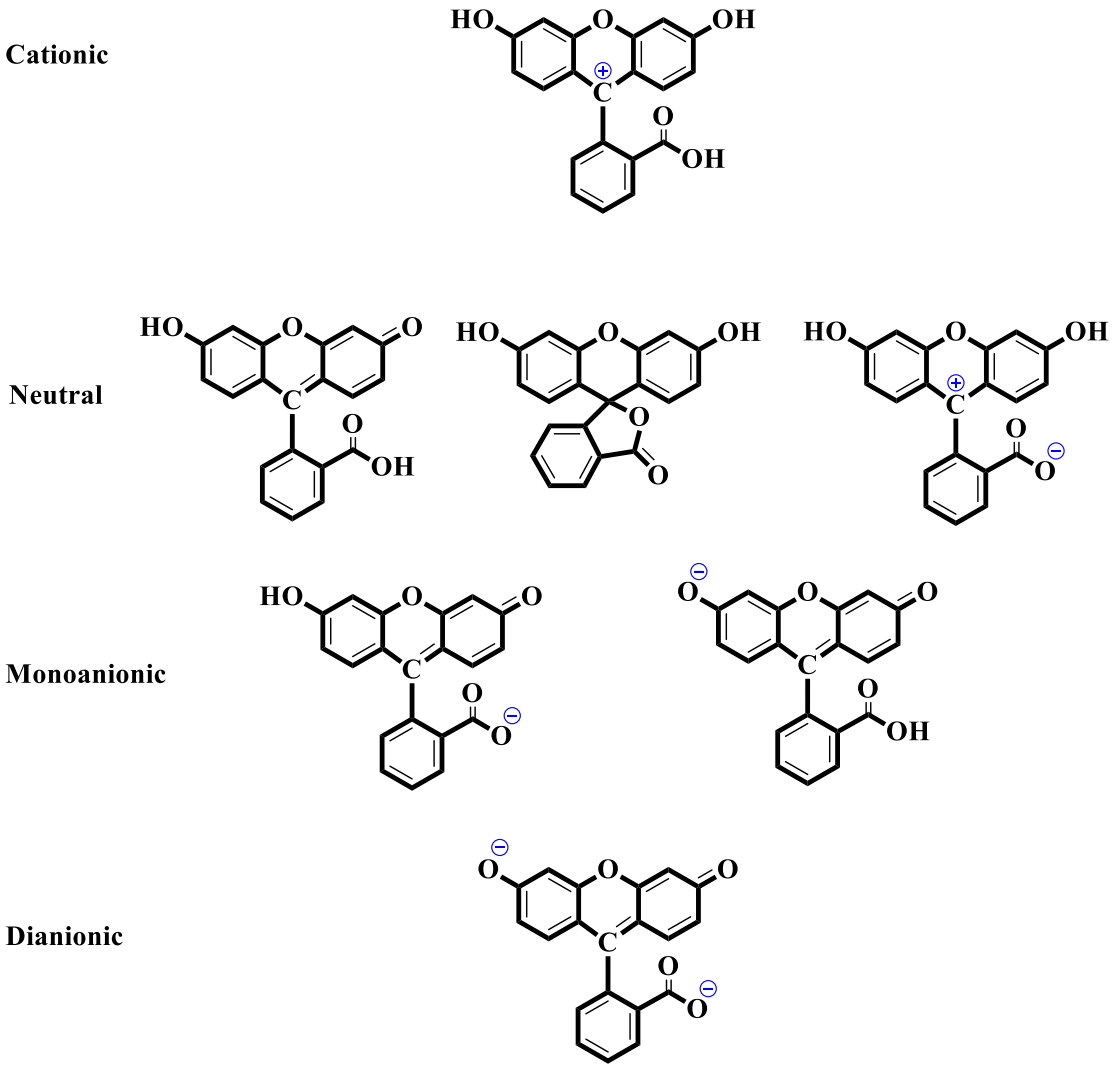

Figure 1.2. Chemical structures of fluorescein at different pH values
(Source: Sjöback et al., 1995)

For ages, a wide variety of fluorescein derivatives have been synthesized and used as fluorescent cores. As shown in figure 1.7, these derivated fluoresceins are 5(6)-carboxyfluorescein **(2)**, 5(6)-carboxyfluorescein succinimidyl ester **(3)**, 5-iodoacetamido fluorescein **(4)**, and fluorescein isothiocyanate (FITC) **(5)**. They are particularly suitable for biological experiments in which fluorescein is covalently attached to materials such as peptides, proteins, nucleotides, oligonucleotides, hormones, drugs, lipids, and other biomolecules (Sun et al., 1997).

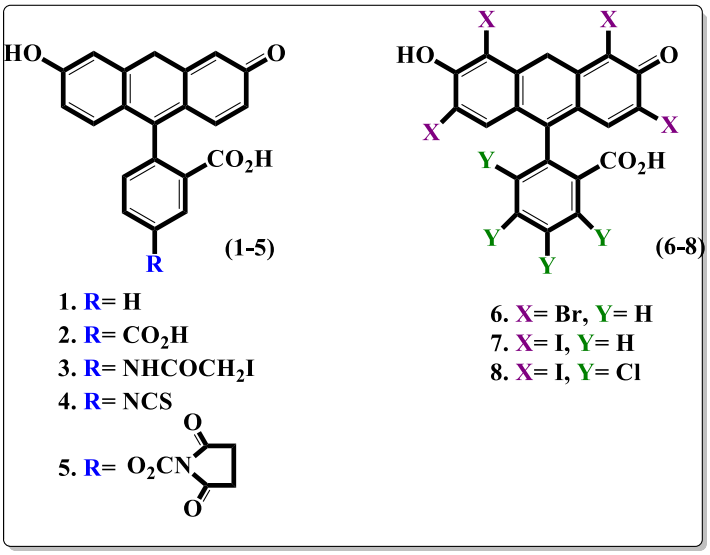

Figure 1.3. Fluorescein Derivatives
(Source: Sun et al., 1997)

Fluorescein as a chemosensor is very worthwhile label because of its high photostability, photochemical and photophysical properties. It has been utilized as a chemodesimeter to determine heavy metals such as Au(II/III), Hg(II), Fe(II/III), Cr(III) in a solution and also cell (Gonçalves, 2007).

Two approaches for the design and synthesis of chemosensors have been reported in previous studies. The first approach uses a chemodosimeter. This term refers to a nonfluorescent probe comprising a fluorophore and a metal ion receptor that produces a new organic molecule that has an exchange in the fluorescence intensity.

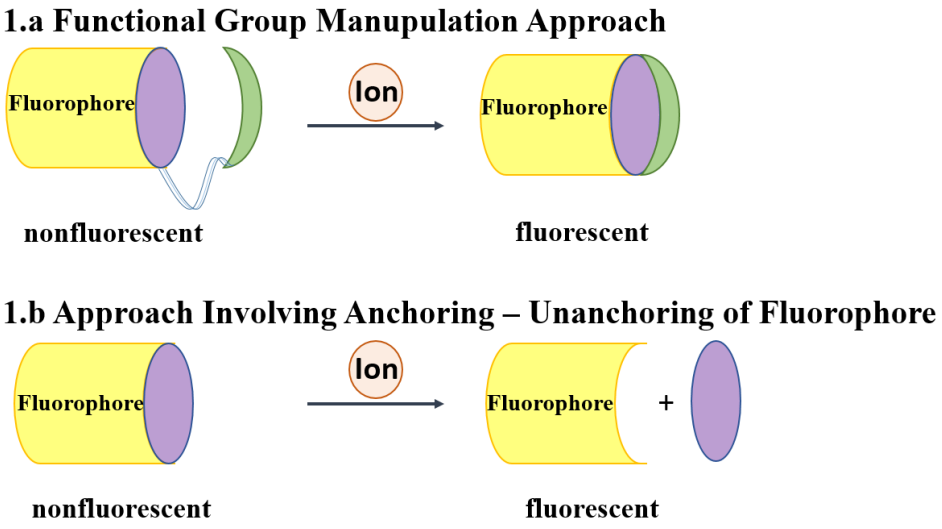

Figure 1.4. Reaction based approach
(Source: Patil et al., 2012)

The second approach is based on complexation wherein a fluorophore and a metal-ion receptor are combined as a non-fluorescent moiety. In the presence of a metal ion, the receptor binds to it and actuates fluorescence intensity.

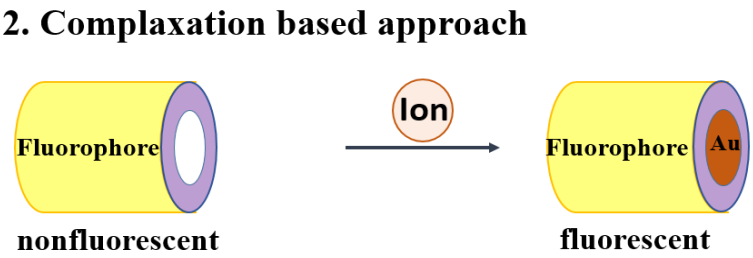

Figure 1.5. Complexation based approach
(Source: Patil et al., 2012)

1.3 Literature studies on sensing Au(III) ion

In many research studies, the alkynophilicity of gold has been exploited in total sensing mechanisms, wherein these mechanisms take advantage of gold's selectivity for alkynes. In 2009, Jou et al. first reported the synthesis of a Au^{3+} selective probe; it is a propargylamide-based sensor made from a rhodamine B alkyne derivative. Studies on the first chemodosimeter for Au^{3+} species exhibited a colorimetric property; i.e., the colour change was visible to the naked eye. The mechanism of action involved the use of a propargylamide moiety to activate the alkynophilicity of Au^{3+}. In the presence of Au^{3+}, the spirolactam was opened and a cyclization reaction occurred from propargylamide to oxazolecarbaldehyde. This sensing mechanism was irreversible, as proven by mass spectroscopy and nuclear magnetic resonance (NMR) measurements. The selective probe was successfully performed on cell cultures.

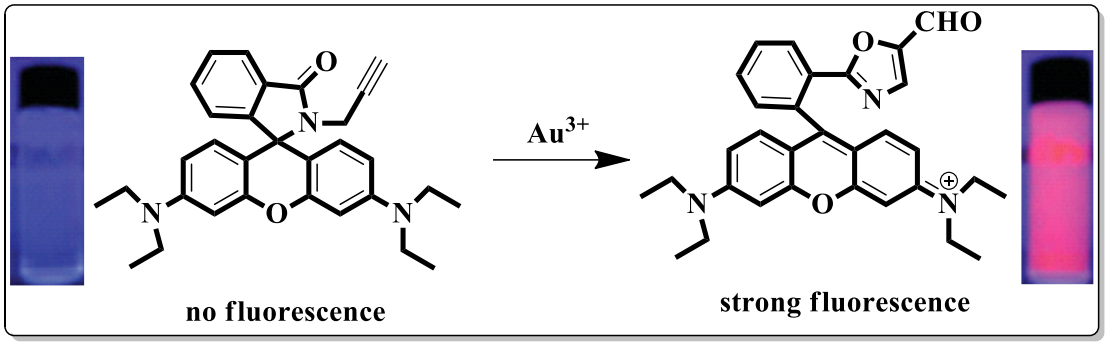

Figure 1.6. Au^{3+}-induced transformation from propargylamide to oxazolecarbaldehyde (Source: Jou et al., 2009)

Simultaneously, another Au^{3+} selective probe was reported in 2009 by Tae and co-workers. Congruently, rhodamine was adopted as a fluorophore and was derivated with an alkyne to utilize gold's alkynophilic properties. A new product, which was not reversible, was obtained; this produced a colour change. This highly sensitive probe was tested with other metal ions; however, no intensity was detected. A biological study was performed in aqueous media, offering a new approach to biological systems.

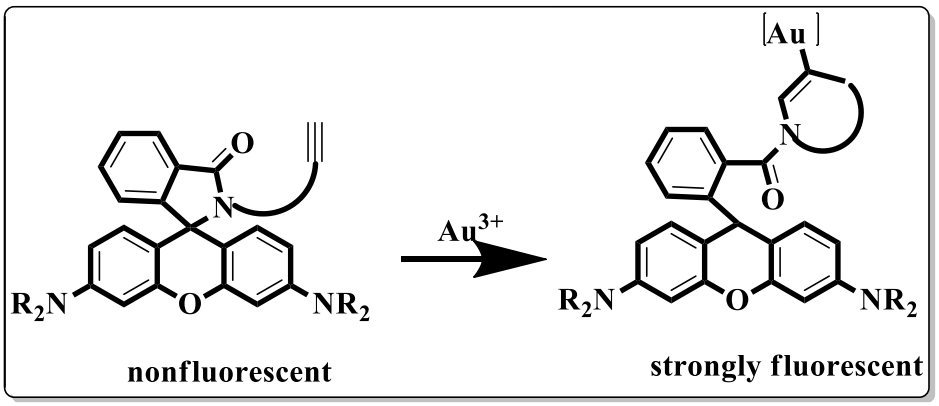

Figure 1.7. Reaction-based fluorescent sensing of gold ions (Source: Yang et al., 2009)

The development of gold-selective fluorescent probes has rapidly gained interest. At the beginning of 2010, the exploration of vinyl gold intermediates presented a pivotal new perspective (Egorova et al., 2010).

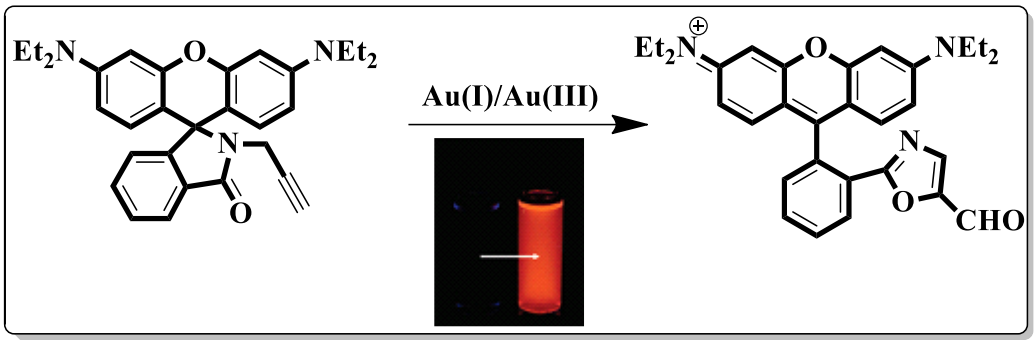

Figure 1.8. Au^{1+}/Au^{3+} promoted sensing process
(Source: Egorova et al., 2010)

Turn-on fluorescent probes, which yielded unexpected products in the sensing mechanism, were developed for $Au^{+}\backslash Au^{3+}$. A similar but different ring-opening reaction was observed. Using characterization, molecule 3 was identified as the major product rather than molecules 1 or 2. To identify the formation mechanism, this process was repeated in non-aqueous media. In dry acetonitrile, molecule 3 could not form in default of nucleophile. An overall cyclization mechanism (shown in Figure 1.9) was proposed. As a result of the above mentioned procedures, a new, efficient gold sensing mechanism was discovered.

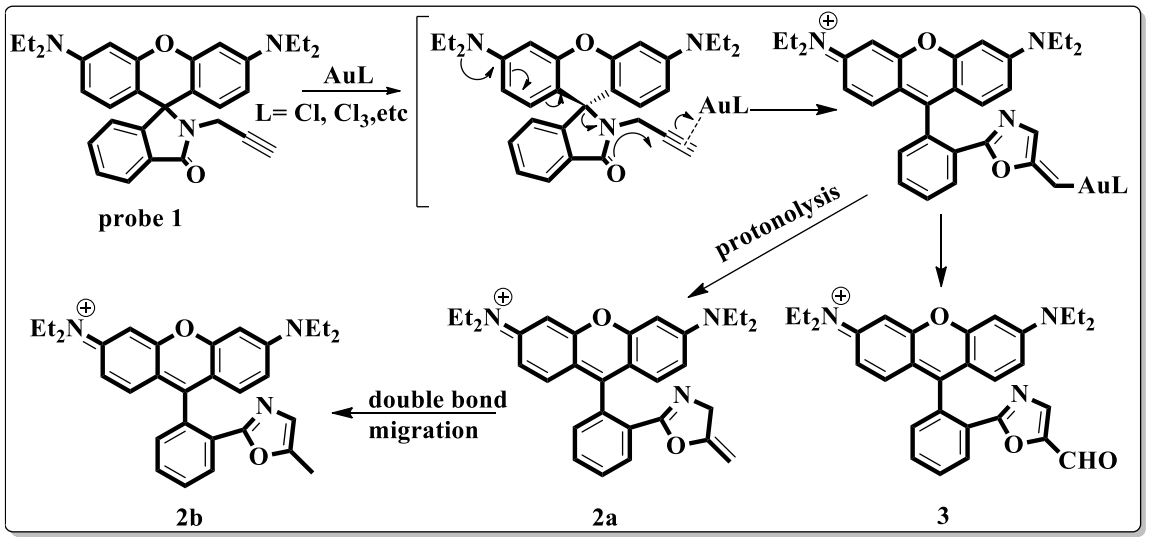

Figure 1.9. Au^{+}/Au^{3+} Promoted spirolactam ring opening of probe 1 to give fluorescent compounds 2 and 3 (Source: Egorova et al., 2010)

Kim and co-workers designed a rational fluorescent probe based on hydroarylation (Do et al., 2010). A compound comprising a vinyl alkyne moiety exhibited

weak fluorescence intensity. After the sensitivity of probe 2 was proven in the presence of trace amounts of Au^{3+} ion; other modified probes were used under the same conditions. As expected, these additional tests emphasized the importance of both the diethylamino and alkyne groups. The developed model was incubated in HaCaT cells, and fluorescence was observed via confocal microscopy.

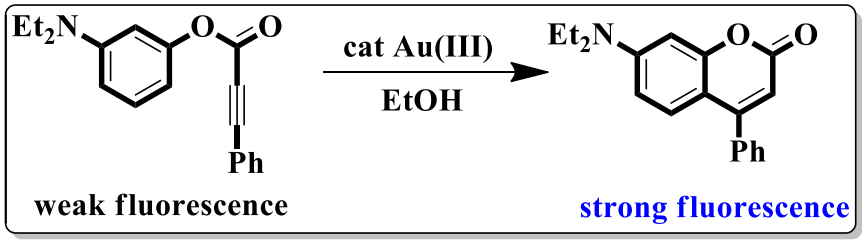

Figure 1.10. Response of the developed probe towards Au^{3+} species
(Source: Do et al., 2010)

In 2012, Ahn and co-workers proposed a spirolactam opening system using (2-Ethynyl) benzoate as a reactive moiety. In this study, fluorescein, which has a structure similar to rhodamine, was used as the fluorophore. The mechanism of this system can be based on a named reaction; moreover, the approach involves anchoring and unanchoring the fluorophore. In this mechanism, a 6-endo cyclization facilitates a fluorescence.

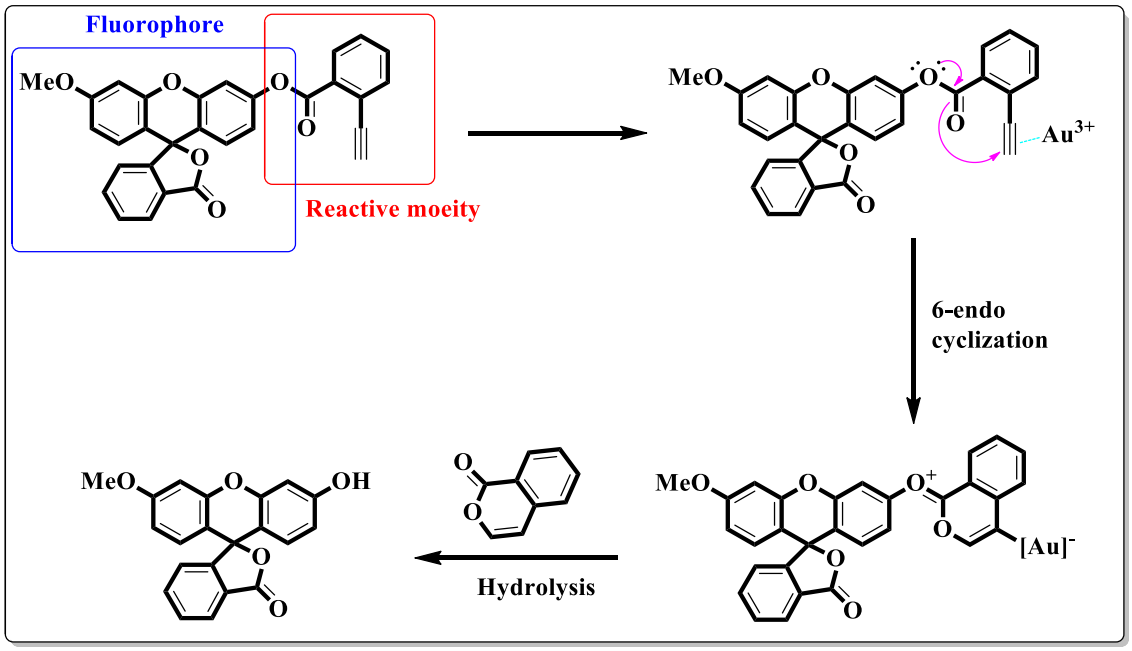

Figure 1.11. Reaction-Based Sensing of Gold Ions
(Source: Seo et al., 2012)

In a more recent example reported by our research group, a rhodamine-based probe was prepared for Au^{+} and Au^{3+} species. Rhodamine-B hydrazide and 2-alkynylbenzaldehyde were used to synthesize the turn-on probe. To determine whether the sensing mechanism was reaction-based or complexation-based, an excess amount of KCN was added to the solution. Following this, no change in colour and no fluorescence could be observed; this proved that an irreversible reaction took place in the sensing system. This reaction-based sensor was demonstrated in living cells, and high fluorescence imaging could be obtained in vitro.

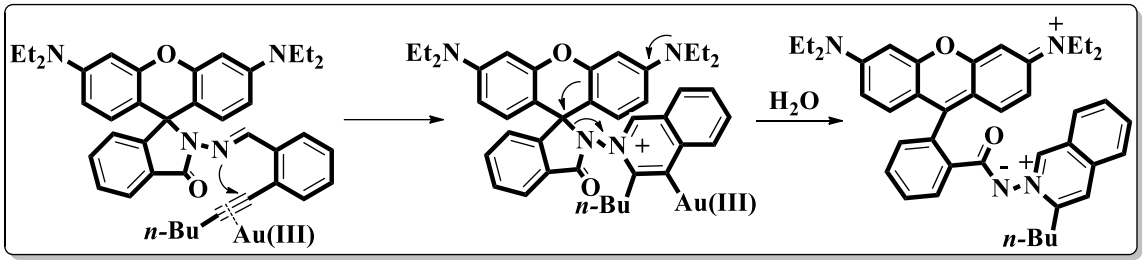

Figure 1.12. Proposed reaction mechanism of Au^{3+} sensing process

(Source: Emrullahoglu et al., 2013)

Previously, several gold-ion sensor molecules have been designed on the basis of various types of chromophores, including coumarin, rhodamine, BODIPY and cyanine. However, there are some drawbacks in these biological systems. In late 2014, a study reported the development of a gold (III) ion selective probe using fluorescein dye. This dye displayed a very high water solubility because of the presence of a hydroxyl group. To synthesize the probe, 4,5-fluoresceindicarboxaldehyde was combined with 1-(pyridin-2-yl)hydrazine; the product obtained was a pink powder. When Au^{3+} was added to the system, a rapid conversion was observed. Moreover, an experiment was performed in different types of solutions. e.g., in pure water, an increase in Au^{3+} acidified the solution media; after adding NaOH, the pH changed again and fluorescence was observed.

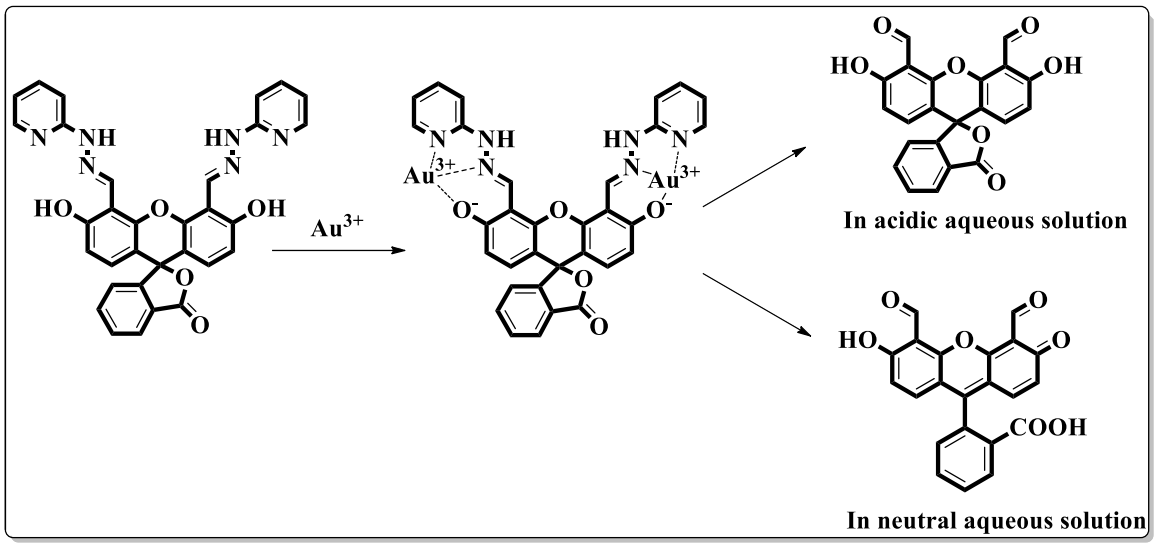

Figure 1.13. Proposed mechanism for the response of 1 to Au^{3+}

(Source: Kambam et al., 2014)

In addition, as a part of ongoing studies, rhodamine and BODIPY dyes were integrated with each other through C=N double bond allowing the differential detection of Hg^{2+} and Au^{3+} (Karakus et al., 2014). Both fluorophores were nonfluorescent before the addition of any metal ions. When the probe was excited at 525 nm in the presence of Au^{3+} ions, a new emission band that belong to the ring opened isomer of rhodamine core was observed. On the contrary, when the same probe was excited at 470 nm, a different emission band which was a characteristic emission band of BODIPY core was obtained. The addition of Hg^{2+} ions to the solution provide that the ring opening cyclization reaction of spirocyclic rhodamine. However, when the solution was excited at 470 nm in the presence of Hg^{2+} ions, no emission bands were reported which means that BODIPY was still in its off mode (Figure 1.14). Meanwhile, the bioimaging applications of the developed molecule were performed with (A549) lung adenocarcinoma cell lines.

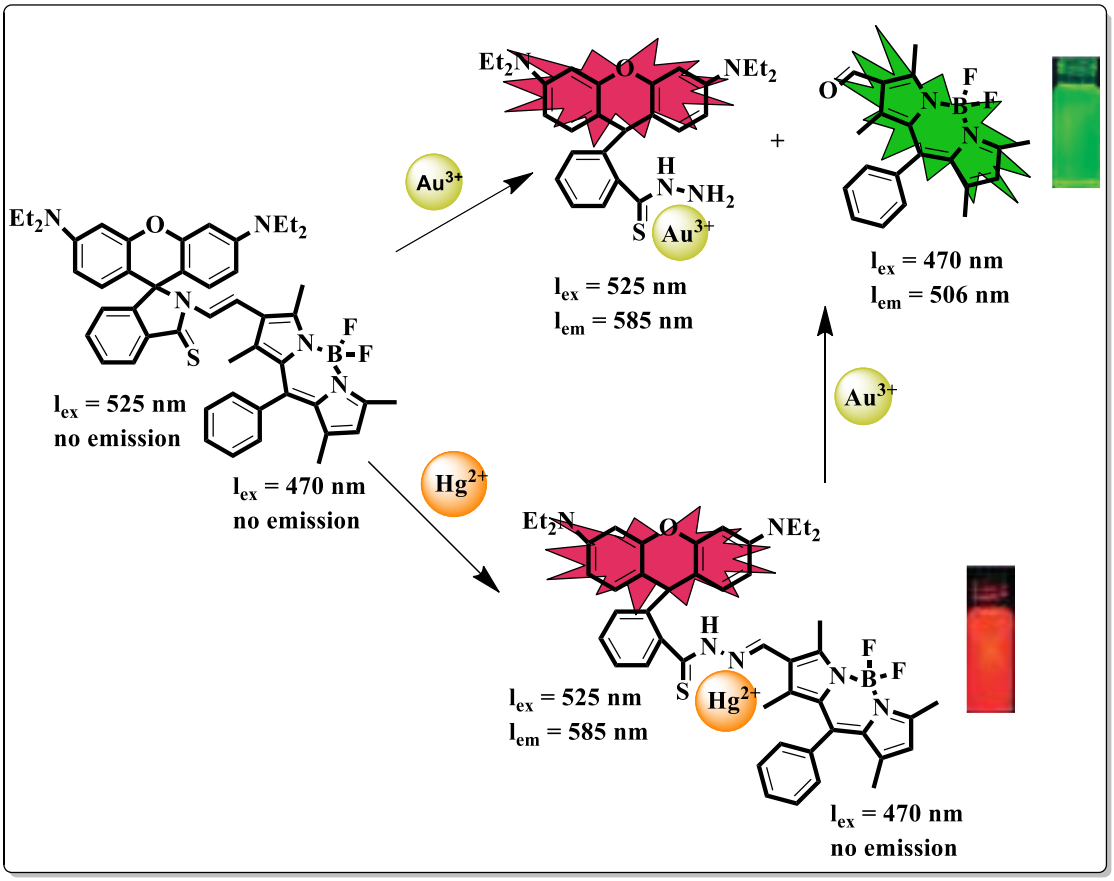

Figure 1.14. Response of the developed probe to the addition of Hg^{2+} and Au^{3+}

(Source: Karakus et al., 2014)

CHAPTER 2

EXPERIMENTAL STUDY

2.1. General Methods

All used reagents were obtained from commercial suppliers (Sigma-Aldrich and Merck) and used without any purification. ^{1}H NMR and ^{13}C NMR spectras were measured on a VNMRJ 400 Nuclear Magnetic Resonance Spectrometer (Varian Medical Systems). UV absorption spectra were obtained with Shimadzu UV-2550 Spectrophotometer and fluorescence measurements were performed by using Varian Cary Eclipse Fluorescence spectrophotometer. Samples were contained in quartz cuvettes with a path length of 10.0 mm (2.0 mL volume). Upon excitation at 460 nm, the emission spectra were integrated over the range 480 nm to 700 nm. The slit width was 5 nm for both excitation and emission. The pH was recorded by HI-8014 instrument (HANNA). All measurements were regulated at least in triplicate.

2.2. Synthesis of Alkynylbenzaldehyde Derivations

The Sonogashira reaction was used to mediate a cross-coupling reaction for the synthesis of alkynylbenzaldehyde derivatives. 2-bromobenzaldehyde was dissolved in 25-ml triethylamine after degassing the solvent with nitrogen gas. To this solution, bis-(triphenylphosphine)palladium(II)dichloride, copper(I) iodide and triphenylphosphine were added. The solution was mixed for 10 min. The alkyne reactant was added to the reaction mixture. Under an inert gas atmosphere, this mixture was stirred under reflux at 50°C. The reaction was monitored by thin layer chromatography (TLC) until the reactant was completely consumed. The product was extracted using dichloromethane and dried using anhydrous $MgSO_4$. The product was purified by column chromatography (100:0.5 Hexane: Ethyl Acetate).

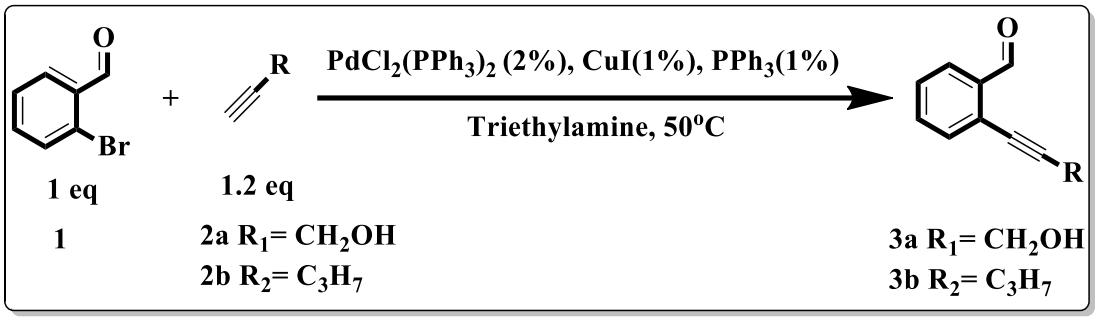

Figure 2.1. Synthesis of alkynylbenzaldehyde derivatives

2.3. Synthesis of Fluorescein Hydrazide

Fluorescein hydrazide **(5)** was synthesized according to the literature procedure (Tae et al., 2009). To solution of 3',6'-dihydroxyspiro[isobenzofuran-1(3H),9'-[9H]xanthen]-3-one in methanol (20 ml), hydrazine hydrate (% 50-60) was injected by dropwise. The reaction was stirred in the reflux system overnight. Consumption of reactant was controlled by the thin layer chromatography. Extraction was done with ethyl acetate and organic layer was dried by using anhydrous $MgSO_4$. The product was purified by column chromatography (100:5 Dichloromethane: Methanol) to able a dark yellow solid.

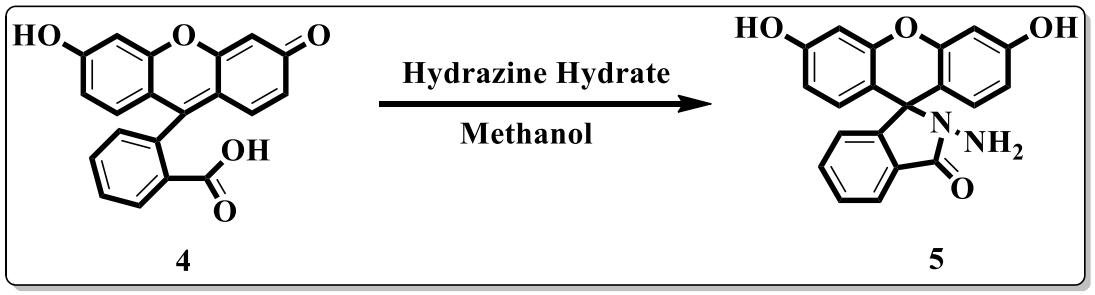

Figure 2.2. Synthesis of fluorescein hydrazide

2.4. Synthesis of Fluorescein Sensors

2.4.1. Synthesis of probe-1 3',6'-dihydroxy-2-((2-(3-hydroxyprop-1-yn-1-yl)benzyl idene)amino)spiro[isoindo line-1,9'-xanthen]-3-one

To a solution of fluorescein hydrazide (5) (114mg, 0.33mmol) in EtOH (10ml), compound 3a (80 mg, 0.50 mmol) was added and stirred at room temperature overnight. When the reaction was completed, this was extracted with dichloromethane (10 ml) three at a time. Obtained organic layer in DCM was dried with anhydrous $MgSO_4$ and concentrated in a vacuum. Purification pathway was carried out by column chromatography (100:1 Dichloromethane: Methanol) in order to afford compound (**probe-1)** as a yellow solid (100mg, %62) ^{1}H NMR (400 MHz, $CDCl_3$) δ: 8.52 (s, 1H), 7.90 (t, J= 9.6 Hz, 2H), 7.40 (quint, J= 6.4 Hz, 2H), 7.20-7.18 (m, 1H), 7.09 (quint, J=8.4 Hz, 2H), 6.95 (d, J=6.4 Hz, 1H), 6.66-6.65 (m, 2H), 6.50-6.48 (m, 2H), 6.38 (dd, J=8.8, 2.0 Hz, 2H), 4.44 (s, 2H). ^{13}C NMR (100 MHz, $CDCl_3$) δ: 165.23, 158.64, 152.07, 151.96, 143.93, 135.63, 133.78, 132.30, 129.32, 128.53, 128.25, 127.75, 127.68, 125.12, 123.57, 123.48, 122.98, 112.63, 109.57, 103.16, 93.76, 81.41, 50.93.

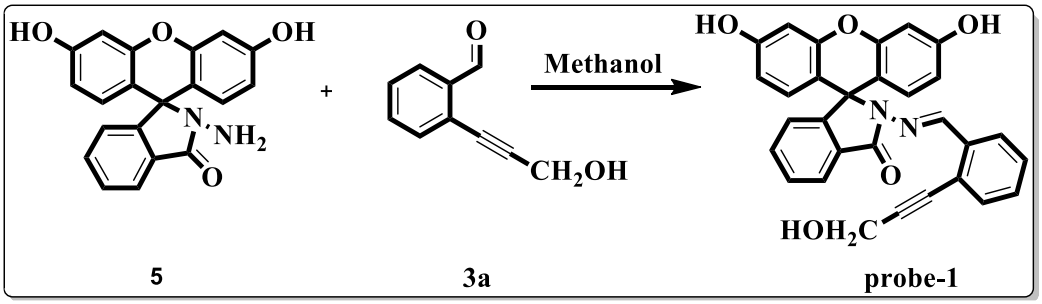

Figure 2.3. Synthesis of **probe-1**

2.4.2. Synthesis of probe-2 3',6'-dihydroxy-2-((2-(pent-1-yn-1yl)benzylidene)amino) spiro[i soindoline-1,9'-xanthen]-3-one

To a solution of fluorescein hydrazide (5) (114mg, 0.33mmol) in EtOH (10ml), compound 3b (86 mg, 0.50 mmol) was added and stirred at room temperature overnight. When the reaction was completed, this was extracted with dichloromethane (10 ml) three at a time. Obtained organic layer in DCM was dried with anhydrous $MgSO_4$ and concentrated in a vacuum. Purification pathway was carried out by column

chromatography (100:1 Dichloromethane: Methanol) in order to afford compound (**probe-2**) as a yellow solid (95mg, %58). ^{1}H NMR (400 MHz, d-DMSO) δ: 9.93 (br.s, 2H), 8.78 (s, 1H), 7.92 (d, J= 7.6 Hz, 1H), 7.73-7.71 (m, 1H), 7.62-7.54 (m, 2H), 7.31-7.29 (m, 3H), 7.08 (d, J=7.6 Hz, 1H), 6.65 (d, J=2.0 Hz, 2H), 6.53-6.51(m, 2H), 6.44 (dd, J= 8.4, 2.0 Hz, 2H), 2.42 (t, J=7.2 Hz, 2H), 1.59 (sextet, J=7.6 Hz, 2H), 1.02 (t, J=7.2 Hz, 3H).^{13}C NMR (100 MHz, d-DMSO) δ: 164.53, 159.13, 152.11, 151.91, 143.99, 135.44, 134.72, 132.95, 130.42, 129.47, 128.63, 127.94, 127.90, 124.26, 123.97, 123.91, 123.83, 112.96, 109.86, 103.09, 96.85, 77.33, 65.11, 22.09, 21.18, 13.96.

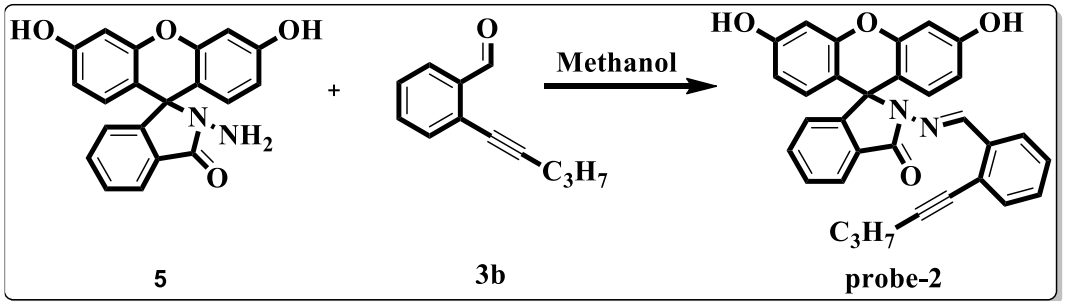

Figure 2.4. Synthesis of **probe-2**

2.5. Cyclization Reactions of Fluorescein Sensors

2.5.1. Synthesis of probe-1P

Probe-1 (40 mg, 0.08 mmol) was dissolved in EtOH/PBS (1.0: 1.0 mL) and $AuCl_3$ (24 mg, 0.06 mmol) was added to the solution. Later, the mixture was stirred at room temperature for 30 minutes. The progress of cyclization reaction was controlled by thin layer chromatography (TLC) and two major products with close R_f values were observed. Despite our great efforts, these two products could not be separated by column chromatography. The ^{1}H NMR spectrum of the product mixture showed the formation of two cyclisation product arising from endo and exo cyclisation, which could yielded six and five membered rings, respectively.

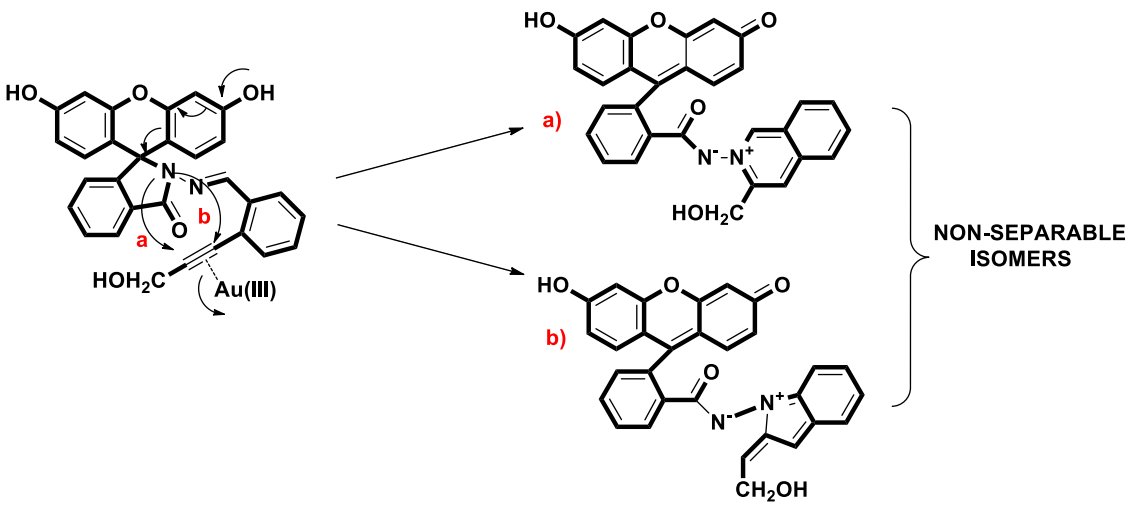

Figure 2.5. Synthesis of **probe-1P**

2.5.2. Synthesis of Probe-2P

Probe-2 (40 mg, 0.08 mmol) was dissolved in EtOH/PBS (1.0: 1.0 mL) and $AuCl_3$ (24 mg, 0.06 mmol) was added to the solution. Later, the mixture was stirred at room temperature for 30 minutes. The progress of cyclization reaction was controlled by thin layer chromatography (TLC) and only one spot was obtained. The mixture solvent was evaporated under reduced pressure that was filtered through celite. Thus column chromatography was done in orde to the purification of product (CH_2Cl_2/MeOH 100:5) to get 34 mg of **probe-2P** (85 %) as yellow solid. ^{1}H NMR (400 MHz, CD_3OD) δ: 8.59 (d, J=8.4 Hz, 1H), 8.35 (s, 1H), 8.21-8.16 (m, 2H), 8.01 (t, J=7.6 Hz, 1H), 7.90-7.79 (m, 3H), 7.71-7.69 (m, 1H), 7.58 (d, J=7.6 Hz, 1H), 6.77-6.70 (m, 4H), 6.32 (s, br, 2H), 3.34-3.31 (m, 2H), 1.69-1.68 (m, 2H), 0.80 (t, J=7.2 Hz, 3H) ^{13}C NMR (100 MHz, CD_3OD) δ: 165.33, 160.69, 154.42, 151.86, 148.26, 145.94, 141.63, 139.01, 137.72, 135.55, 130.52, 130.25, 129.59, 129.40, 129.02, 128.91, 128.71, 125.89, 125.60, 124.72, 113.06, 108.38, 103.16, 35.60, 21.25, 13.21. HRMS: m/z: Calcd. for ($C_{32}H_{24}N_2O_4$) $(M)^+$: 500.1753; found, 500.1753.

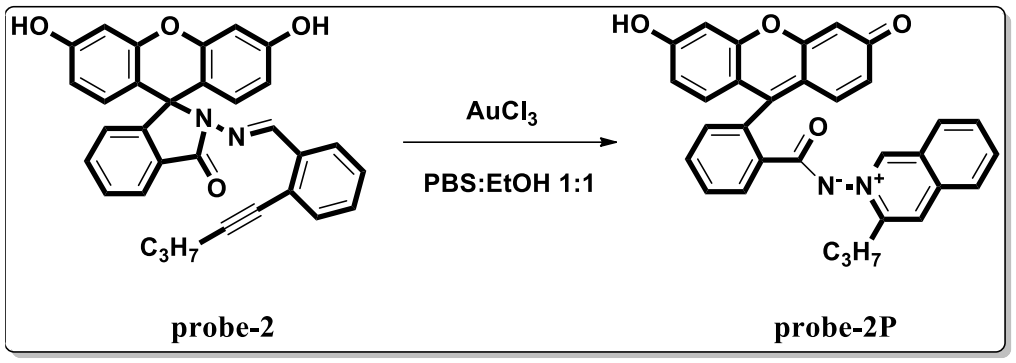

Figure 2.6. Synthesis of **probe-2P**

CHAPTER 3

RESULTS AND DISCUSSION

In this study, a new Au^{3+} ion sensor based on a fluorescein dye modified with an alkyne moiety was developed. Several selective probes have been designed and synthesized the over last years. However, optimizing the detection conditions to achieve maximum fluorescence intensity is a challenge. While most of the probes require organic solvents, probes which are soluble in aqueous buffer solutions are highly desirable. Thus, different buffer solutions, such as HEPES, PBS and phosphate buffers, were evaluated; it was found that a 10 μM dye dissolved in a 10 mM PBS buffer was a very suitable sensing medium. As expected, **probe-1** was not fluorescent in the buffer system due to its ring closed spirocyclic structure. Moreover, after the addition of $AuCl_3$ (10 μM), the solution (pH = 7, 10 mM PBS buffer) turned yellow and emitted green light under UV light.

Figure 3.1. Fluorescence image of **probe-1** + Au^{3+}

In this section, all spectroscopic measurements were performed for two different probe structures and their spectroscopic behaviours were compared systematically.

3.1. Spectroscopic Results of Probe-1

Spectroscopic measurements were carried out in a 10 mM PBS buffer solution. The effect of pH was evaluated in the pH range 2–12. As known from the literature, the detection system did not work in the acidic media because of the fluorescein-based dye structure. When the pH reached 7, fluorescence was observed, which gradually increased in basic media. However, the fluorescence intensity decreases above pH 9. Consequently, it was concluded that a pH value of 7 is viable, which is also significant for application in cell-based studies.

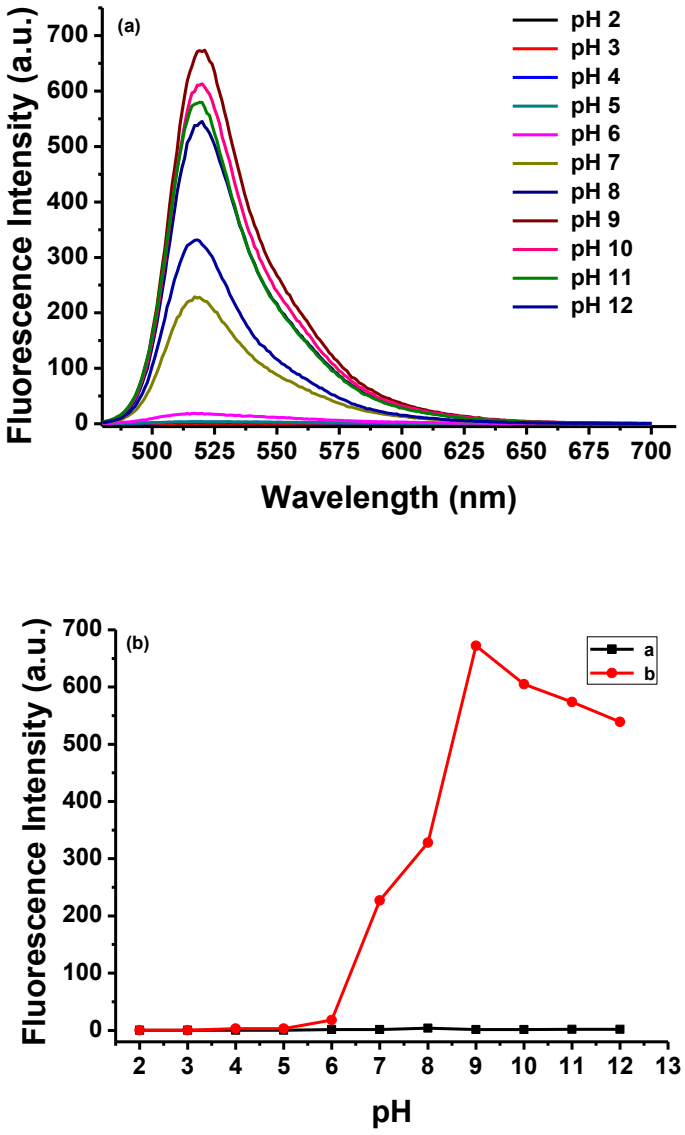

Figure 3.2. Effect of pH on the fluorescence intensity of **probe-1** (10 μM) in PBS a; in absence of Au^{3+}, b; in presence of Au^{3+} (5 equiv.)

It can be seen from Figure 3.3 that **probe-1** (10 μM) is colourless in PBS buffer, which implies that it has any intensity. However, with the addition of 5 equivalents of Au^{3+} ions to the solution absorbance intensity increases and the solution turns into light yellow. Concurrently, there is a 300-fold increase in fluorescence intensity compared to the solution fluorescence in the absence of Au^{3+} ions.

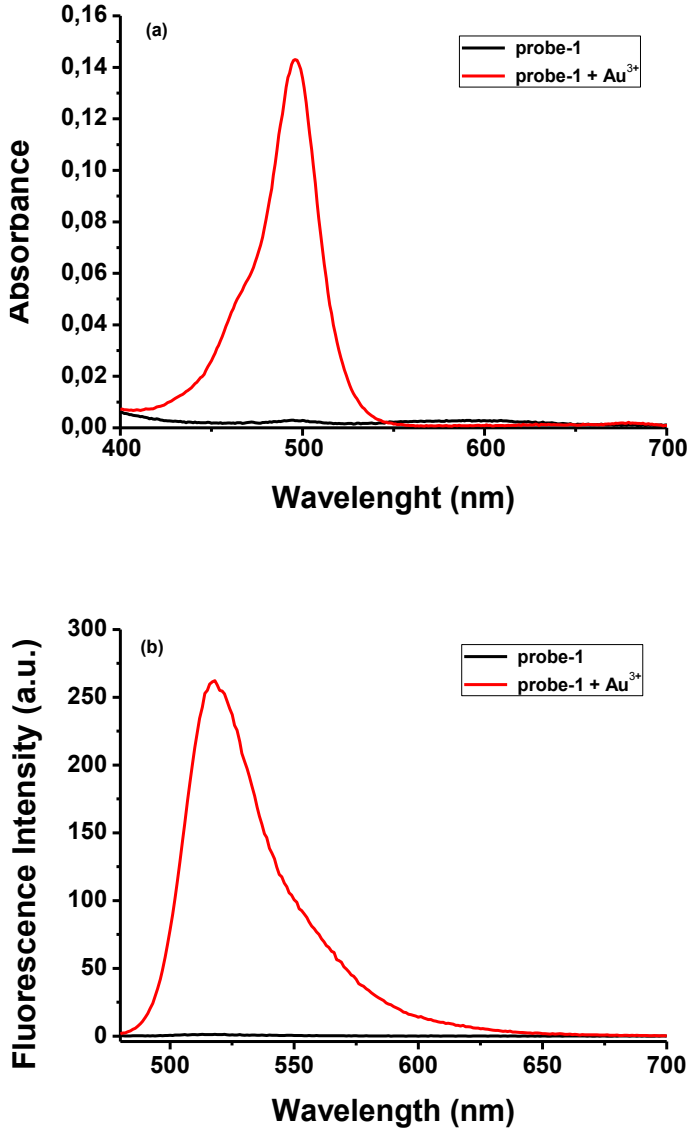

Figure 3.3. (a) Absorption and (b) emission spectra of **probe-1** (10 μM) and Au^{3+} (5.0 equiv.) in PBS at pH = 7.0; (λ_{ex}: 460 nm, at 25 ◦C)

The rate of the reaction was then evaluated. In the presence of Au^{3+} ions, a significant increase in the fluorescence intensity was observed in a very short time. The fluorescence continued to increase for approximately 15 min before stabilizing. Based on

this, all measurements were carried out after 15 min, allowing the fluorescence signal to saturate.

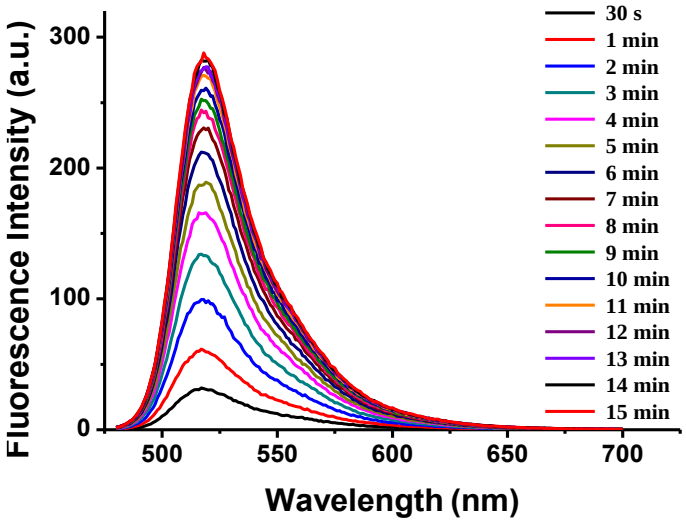

Figure 3.4. Time-dependent fluorescence change of **probe-1** (10 μM) in the presence of an 5.0 equivalent of Au^{3+} measured in PBS at pH = 7.0

Titration of **probe-1** (10 μM) with Au^{3+} ions shows that the increase in emission intensity is linear with an increase in the concentration of Au^{3+} ions (mole equivalents 1–10). After the addition of 6 equivalents of Au^{3+} ions, the system became saturated and the fluorescence intensity became stable (Figure 3.5).

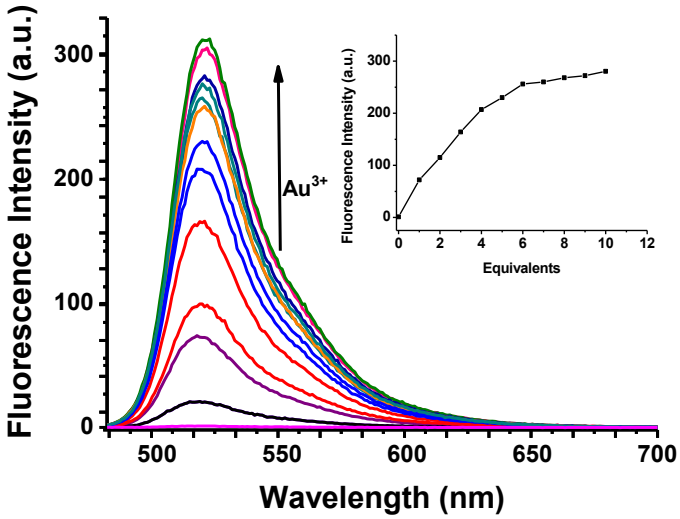

Figure 3.5. Fluorescence spectra of **probe-1** (10 M) in PBS at pH = 7.0 in the presence of Au^{3+} (mole equivalents = 0–10)

The selectivity of **probe-1** was determined by titrating it with an excess amount of various metal cations under optimum conditions. Crucially, **probe-1** demonstrated no spectral response to alkynophilic metal ions such as Au^{+}, Ag^{+}, Ni^{2+}, Pd^{2+}, Fe^{3+} and Hg^{2+}, among others. Moreover, the probe can distinguish between the different oxidation states of gold, namely Au^{+} and Au^{3+}. As it is well established, Au^{3+} ions prefer to interact with thiol species. For this reason, it can be highly challenging to discriminate between different gold species in a biological environment. Thus, examining the response of the fluorescent probe towards Au^{3+} ions in the presence of reactive biothiol species, such as cysteine (one of the most nucleophilic and chemically reactive among the amino acids), is essential. The detection of Au^{3+} ions was carried out in the presence of several biothiols in solution (Figure 3.6).

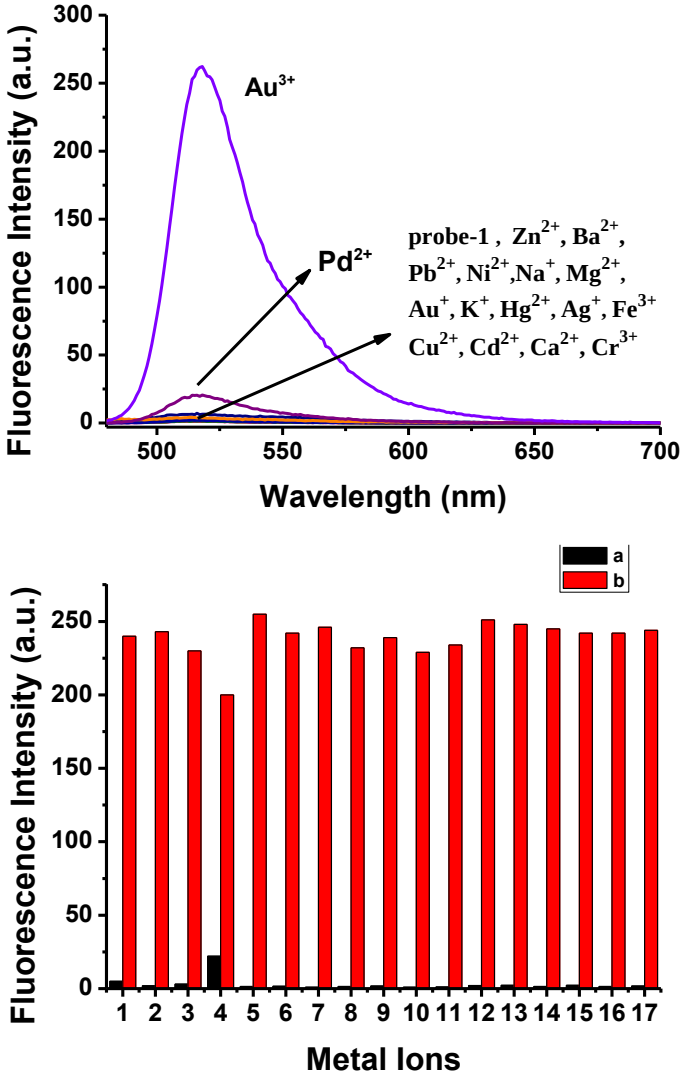

Figure 3.6. (a) Fluorescence intensities of **probe-1** (10 μM) in PBS at pH = 7.0 in the presence Au^{3+} (5.0 equiv.) and 20.0 equivalent of the cations interest (b)

Fluorescence intensities of **probe-1** (10 µM) in PBS at pH = 7.0 in presence of 20.0 equivalents of the cations (black bar); in presence of cations and Au^{3+} (5.0 equiv.) (red bar); 1, Au^{+}; 2, Ag^{+}; 3, Cd^{2+}; 4, Pd^{2+}; 5, Cr^{3+}; 6, Cu^{2+}; 7, Fe^{3+}; 8, Hg^{2+}, 9, K^{+}; 10, Ca^{2+}; 11, Mg^{2+}; 12, Na^{+}; 13, Ni^{2+}; 14, Pb^{2+}; 15, Ba^{2+}; 16, Zn^{2+}; 17, Cysteine.

After all optimization study, to calculate detection limit of the **probe-1** fluorescence titration was done carefully. In order to determine the S/N ratio, the emission intensity of **probe-1** (10 µM) was measured by 10 times and the standard deviation of these blank measurements was determined. A good linear relationship between the fluorescence intensity and Au^{3+} ion concentration was obtained in range 0 – 0,1 µM (R = 0.990) (Figure 3.7). The detection limit was then calculated with the equation:

Detection Limit = 3σbi/m

σbi is the standard deviation of blank measurements;

m is the slope between intensity versus sample concentration.

The detection limit was measured as 11 nM at S/N = 3.

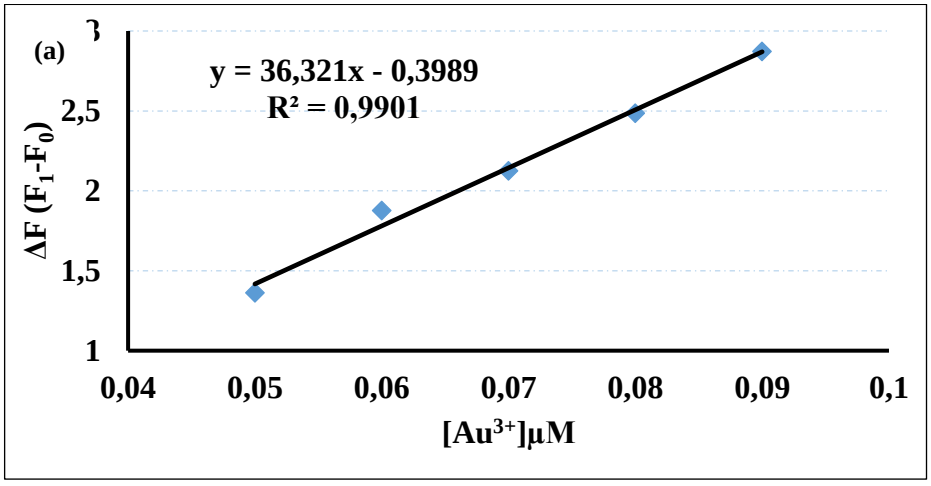

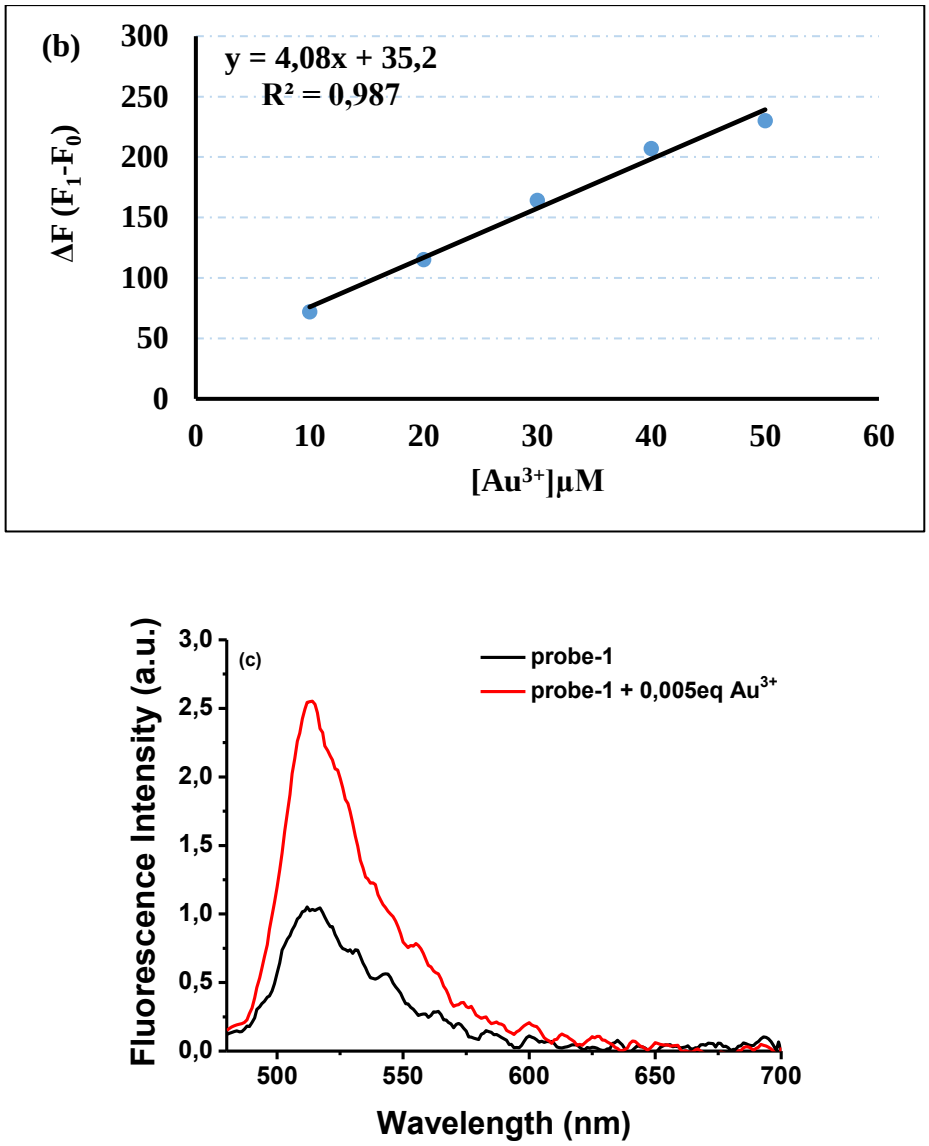

Figure 3.7. (a) Fluorescence changes of **probe-1** (10 µM) upon addition of Au^{3+} (0.005 to 0.01 equiv.) (b) Fluorescence changes of upon addition of Au^{3+} (1 to 5 equiv.) (c) Fluorescence spectra of **probe-1** (10 µM) in the presence of Au^{3+} (0.005 equiv.) in PBS at pH = 7.0

The product of the reaction between **probe-1** and Au^{3+} was isolated to identify the mechanism of the reaction. The progress of this reaction was monitored by TLC. Two major products with close R_f values in TLC were identified. Despite our efforts, the products could not be separated by column chromatography. However, ^1H NMR

spectrum of the mixture showed the formation of two cyclization products, which contain a five- and six-membered ring.

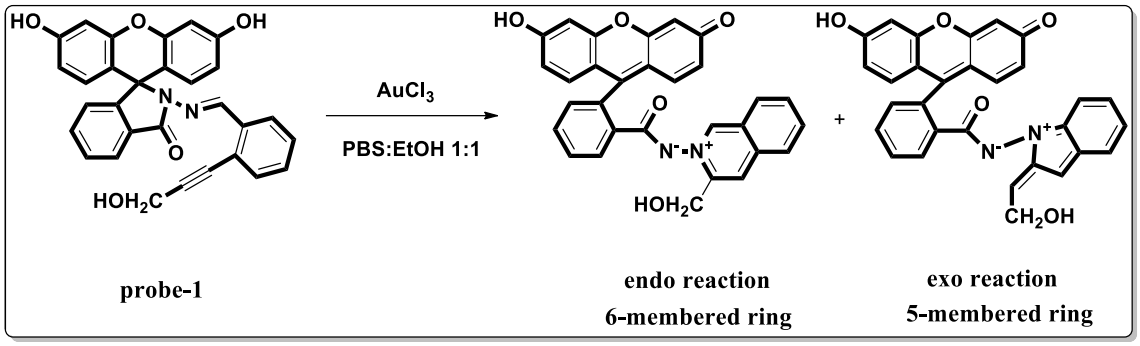

Figure 3.8. Cyclization reaction of **probe-1**

Alternatively, to confirm the reaction mechanism, **probe-2**, which has similar alkynyl moiety, was synthesized. The optimization studies were performed under identical detection conditions to **probe-2** and a high fluorometric response was obtained. Identification of the detection mechanism was confirmed by ^{1}H NMR, ^{13}C NMR and high-resolution mass spectral analysis.

3.2. Spectroscopic Results of Probe-2

In the previous spectroscopic measurements, solvent system was a 10 mM PBS buffer solution. Next, the effect of pH was scanned in the range from 2 to 12. Indistinguishably, **probe-2** behaved similar to **probe-1**.

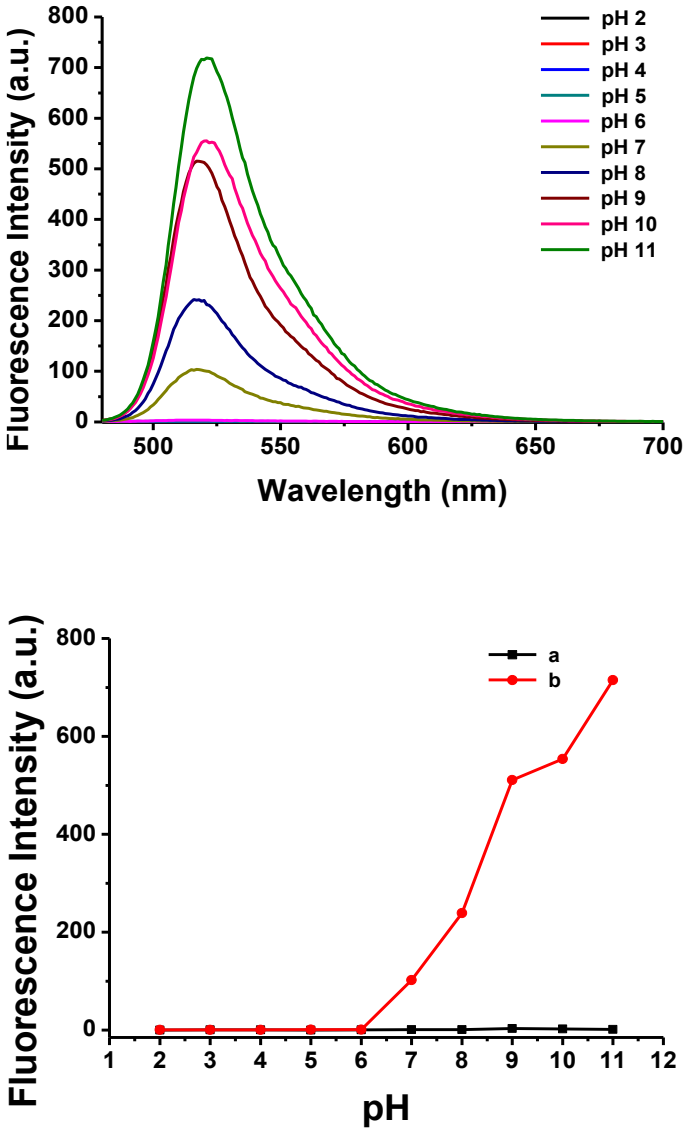

Figure 3.9. Effect of pH on the fluorescence intensity of **probe-2** (10 μM) in PBS a; in absence of Au^{3+}, b; in presence of Au^{3+} (5 equiv.)

Difference between absence and presence of Au^{3+} ion was determined for **probe-2** spectroscopically. Colourless solution gave intensity as a result of the addition of Au^{3+} (5equiv.). Likewise, **probe-2** gained fluorescent property that so it had 100 fold increase in fluorescence intensity.

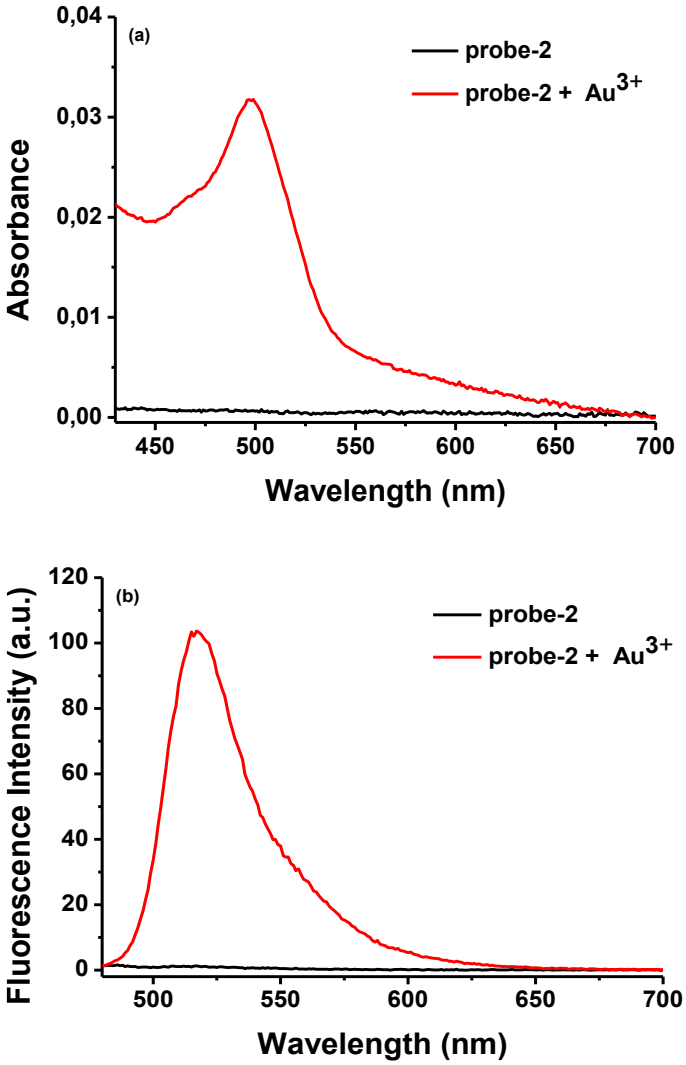

Figure 3.10. (a) Absorption and (b) emission spectra of **probe-2** (10 μM) and Au^{3+} (5.0 equiv.) in PBS at pH = 7.0; (λ_{ex}: 460 nm, at 25 ◦C)

To examine the properties of **probe-2**, time dependent fluorescence change was measured under specified conditions. It was adjusted that probe reached to be saturated in 15 minutes.

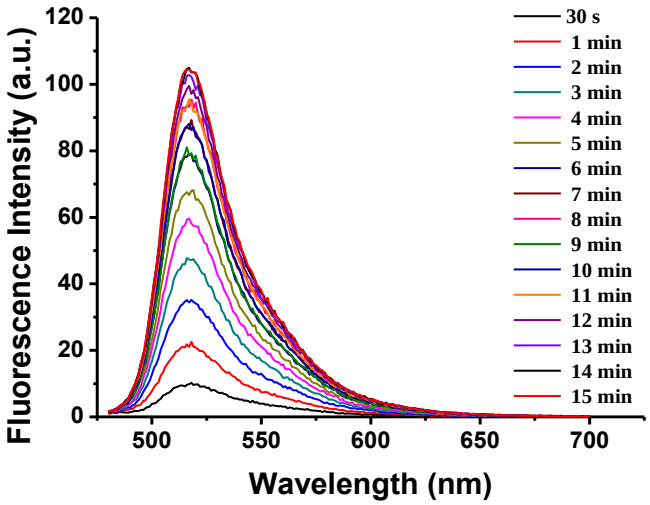

Figure 3.11. Time-dependent fluorescence change of **probe-2** (10 μM) in the presence of an 5.0 equivalent of Au^{3+} measured in PBS at pH = 7.0

Titration of **probe-2** (10 μM) with Au^{3+} picked out that emission intensity remains linearly with the increase in concentration of Au^{3+} (mole equivalents 1-13). After the addition of 11 equivalents of Au^{3+} ions, the system became saturated, gained stability in the fluorescence intensity (Figure 3.12).

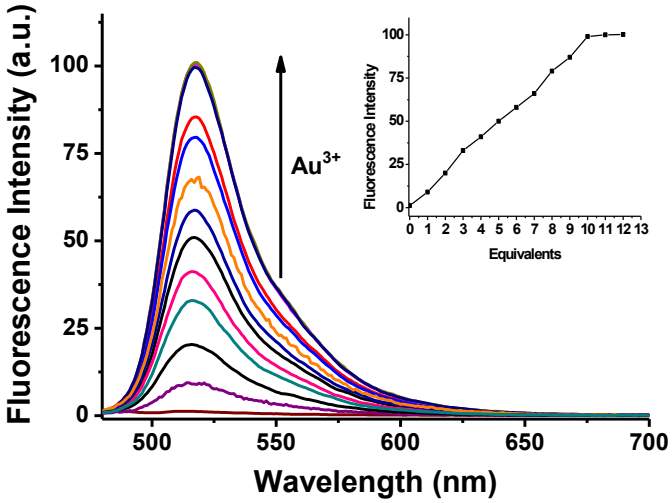

Figure 3.12. Fluorescence spectra of **probe-2** (10 M) in PBS at pH = 7.0 in the presence of Au^{3+} (mole equivalents = 0–10)

In the last part of measurements, selectivity of **probe-2** toward Au^{3+} was determined in presence of many cations and thiols. As seen in figure 3.13, **probe-2** did

not response to any others except Au^{3+} ion. And then, fluorescence intensity increased by 100 fold when Au^{3+} (5 equiv.) was added to the prepared solutions.

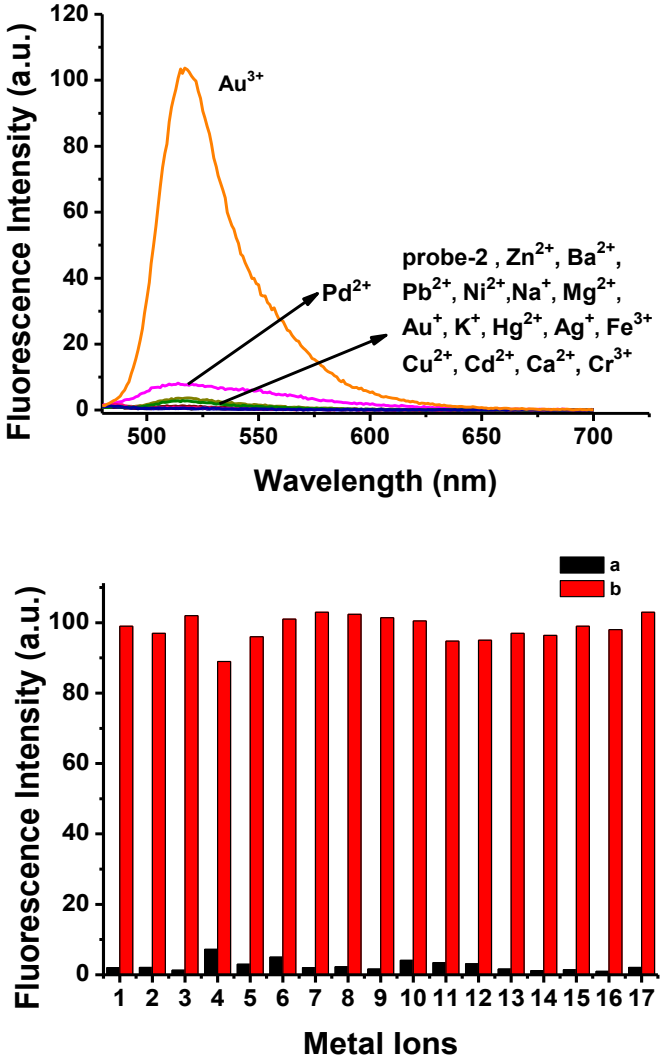

Figure 3.13. (a) Fluorescence intensities of **probe-2** (10 μM) in PBS at pH = 7.0 in the presence Au^{3+} (5.0 equiv.) and 20.0 equivalent of the cations interest (b) Fluorescence intensities of **probe-2** (10 μM) in PBS at pH = 7.0 in presence of 20.0 equivalents of the cations (black bar); in presence of cations and Au^{3+} (5.0 equiv.) (red bar); 1, Au^{+}; 2, Ag^{+}; 3, Cd^{2+}, 4, Pd^{2+}; 5, Cr^{3+}; 6, Cu^{2+}; 7, Fe^{3+}; 8, Hg^{2+}, 9, K^{+}; 10, Ca^{2+}; 11, Mg^{2+}; 12, Na^{+}; 13, Ni^{2+}; 14, Pb^{2+}; 15, Ba^{2+}; 16, Zn^{2+}; 17, Cysteine.

3.3. Cell Imaging of Probe-1

In result of the purposed study, the molecules were developed as favourable in cell culture. The probes demonstrate high solubility in aqueous media, a low detection limit and rapid response. To that end, human lung adenocarcinoma cells (A549) were

incubated with **probe-1** (10 μM) at 37°C for 20 min. Furthermore, a 50 μM Au^{3+} solution was added and the cells were incubated for 20 min. After staining with DAPI (1.0 mM), fluorescence images were acquired in the absence and presence of Au^{3+} ions. The acquired cell images showed that cells were healthy and did not display any change in their morphology.

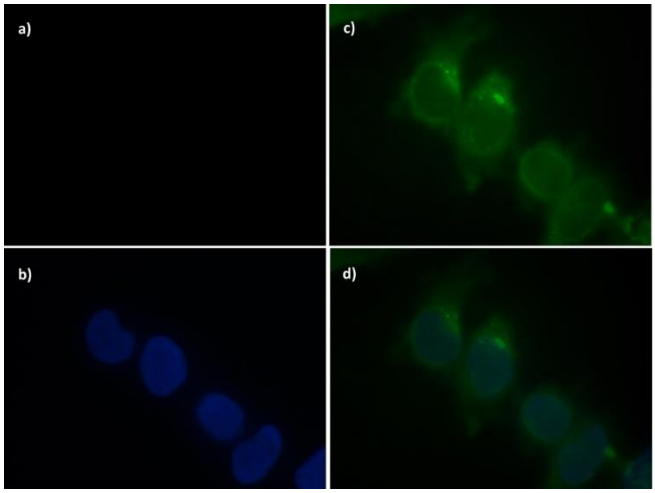

Figure 3.14. Images of A-549 (Human lung adenocarcinoma) cells: a) Cells were incubated with **probe-1** (10 M) in the absence of Au^{3+} b) cells are detected with DAPI nuclear counter-stain (control) c) cells were incubated with **probe-1** (10 M) and Au^{3+} (50 M) d) merged images of frame (b) and (c) DAPI blue, **probe-1** green.

CHAPTER 4

CONCLUSION

New fluorescent probes for the detection of Au^{3+} species were developed; these probes gave a rapid response with high intensity in aqueous media. The turn-on fluorescent probes were used effectively in spectroscopic measurements and cell-imaging applications.

Probe-1 contained fluorescein as a fluorophore, which was derivatized with a propargyl alcohol functionality. Although this probe showed high selectivity and sensitivity, the cyclization products could not be determined. To gather evidence about the mechanism, an alternative fluorescent probe was designed, which also gave good results for spectroscopic measurements. These two probes showed similar response times and selectivities. However, as expected, a comparison of the fluorescence intensities of **probe-1** and **probe-2** showed that **probe-1** exhibited higher intensity. Because of the presence of a hydroxyl group, **probe-1** gained higher solubility in pure aqueous media; this resulted in a fluorescence intensity with a 300 fold enhancement factor. According to measurements, Au^{3+} species could be detected at very low concentrations (LoD= 11 nM).

Cell-imaging applications for monitoring Au^{3+} ions in solution and living cells was studied successfully. No fluorescence was observed in the cells before the addition of gold species; however, upon incubation with Au^{3+}, the cells started to emit a fluorescence emission and it was concluded that the probe was able to pass through the cell membrane and detected Au^{3+} ions in cell lines.

REFERENCES

Chae, M.-Y.; Czarnik, A. W. Fluorimetric Chemodosimetry Mercury(II) and Silver(I) Indication in Water via Enhanced Fluorescence. J. Am. Chem. Soc. 1992, 114, 9704-9705.

Gonçalves, S. Fluorescent Labeling of Biomolecules with Organic Probes. Chem. Rev. 2009, 109, 190–212.

Yang, Y.-K; Lee, S.; Tae, J. A Gold (III) Ion-Selective Fluorescent Probe and Its Application to Bioimagings. Org. Lett. 2009, 11, 5610-5613.

Jou, M. J.; Chen, X., Swamy, K.-M.-K.; Kim, H. N.; Kim, H.-J.; Lee, S. L.; Yoon, J. Highly Selective Fluorescent Probe for Au^{3+} Based on Cyclization of Propargylamide. Chem. Commun. 2009, 7218–7220.

Egorova, O. A.; Seo, H.; Chatterjee, A.; Ahn, K. H. Reaction-Based Fluorescent Sensing of Au(I)/Au(III) Species: Mechanistic Implications on Vinylgold Intermediates. Org. Lett. 2010, Vol. 12, No. 3, 401-403.

Do, J. H.; Kim, H. N.; Yoon, J.; Kim, J. S.; Kim, H.-J. A Rationally Designed Fluorescence Turn-On Probe for the Gold (III) Ion. Org. Lett. 2010, Vol. 12, No. 5, 932-934.

Dong, M.; Wang, Y.-W.; Peng, Y. Highly Selective Ratiometric Fluorescent Sensing For Hg^{2+} and Au^{3+}, Respectively, in Aqueous Solution. Org. Lett. 2010, 12, 5310-5313.

Yuan, L.; Lin, W.; Yang Y.; Song J. A Fast-Responsive Fluorescent Probe for Detection of Gold Ions in Water and Synthetic Products. Chem. Commun. 2011, 47, 4703–4705.

Seo, H.; Jun, M. E.; Egorova, O. A.; Lee, K. H.; Kim, K.-T.; Ahn, K. H. A Reaction-Based Sensing Scheme for Gold Species: Introduction of a (2-Ethynyl) benzoate Reactive Moiety. Org. Lett. 2012, Vol. 14, No. 19, 5062-5065.

Patil, N. T.; Shinde, V. S.; Thakare, M. S.; Kumar, P. H.; Bangal, P. R.; Barui, A. K.; Patra, C. R. Exploiting the higher alkynophilicity of Au-species: development of a highly selective fluorescent probe for gold ions. Chem. Commun. 2012, 48, 11229–11231.

Emrullahoglu, M.; Karakus, E.; Ucuncu, M. A Rhodamine Based Turn-on Chemodosimeter For Monitoring Gold Ions in Synthetic Samples and Living Cells. Analyst, 2013, 138, 3638-3641.

Choi, J. Y.; Kim, G.-H.; Guo, Z.; Lee, H. Y.; Swamy, K. M. K., Pai, J.; Shin, S.; Shin, I.; Yoon, J. Highly Selective Ratiometric Fluorescent Probe for Au3+ and Its Application to Bioimaging. Biosens. Bioelectron. 2013, 49, 438– 441.

Oztas, Z.; Pamuk, M.; Algi, F. Nonreaction-based Fluorescent Au3 Probe that Gives Fast Response in Aqueous Solution. Tetrahedron Lett. 2013, 69, 2048-2051.

Karakus, E.; Ucuncu, M.; Emrullahoglu, M. A Rhodamine/BODIPY-Based Fluorescent Probe For the Differential Detection of Hg(II) and Au(III). Chem. Commun. 2014, 50, 1119-1121.

Ucuncu, M.; Emrullahoglu, M. a BODIPY-Based Reactive Rrobe for the Detection of Au(III) Species and Its Application to Cell Imaging. Chem. Commun. 2014, 50, 5884-5886.

Kambam, S.; Wang, B.; Wang, F.; Wang, Y.; Chen, H.; Yin, J.; Chen, X. A Highly Sensitive and Selective Fluorescein-Based Fluorescence Probe for Au^{3+} and Its Application in Living Cell Imaging. Sens. Actuators 2015, B 209, 1005–1010.

Yang, Y.; Yin, C.; Huo, F.; Chao, J. A Selective Fluorescent Probe for Detection of Gold (III) Ions and Its Application to Bioimaging. RSC Adv. 2013, 3, 9637–9640.

Canturk, C.; Ucuncu, M.; Emrullahoglu, M. A BODIPY-Based Fluorescent Probe for the Differential Recognition of Hg(II) and Au(III) Ions. RSC Adv. 2015, 5, 30522–30525.

Ucuncu, M.; Karakus, E.; Emrullahoglu, M. A BODIPY/Pyridine Conjugate for Reversible Fluorescence Detection of Gold(III) Ions. New J. Chem. 2015, 39, 8337-8341.

Yang, X.; Liu, X.; Li, Y.; Wu, F.; Mao, J.; Yuan, Y.; Cui, Y.; Sun, G.; Zhang, G. A Differentially Selective Probe Based on Diketopyrrolopyrrole With Fluorescence turn-on Response to Fe3, and dual-mode turn-on and Ratiometric Response to Au^{3+} , and Its Application in Living Cell Imaging. Biosens. Bioelectron. 2016, 80, 288–293.

Kang, S.; Kim, S.; Yang, Y.-K.; Bae, S.; Tae, J. Fluorescent and Colorimetric Detection of Acid Vapors by Using Solid-Supported Rhodamine Hydrazides. Tetrahedron Lett. 2009, 50, 2010–2012.

Sjöback, R.; Nygren, J.; Kubista, M. Absorption and Fluorescence Properties of Fluorescein. Spectro. Acta Part 1995, A51, L7-L21.

Braun, I.; Asiri, A. M.; Hashmi, A. S. K. Gold Catalysis 2.0. ACS Catal. 2013, 3, 1902 −1907.

Dorel, R.; Echavarren, A. M. Gold (I)-Catalyzed Activation of Alkynes for the Construction of Molecular Complexity. Chem. Rev. 2015, 115, 9028 −9072.

Wanga, Y.; Liua, Y.-W.; Miaoa, J.-F.; Rena, M.-H.; Guo, W.; Lv, X. A Novel BODIPY Based Fluorescent Probe for Au3+ Ions with High Selectivity and Its Application to Bioimaging. Sens. Actuators B: Chem. 2016, Vol.226, 364–369.

Yim, D.; Yoon, H. N.; Lee, C.-H.; Jang, W. D. Light-Driven Au(III)-Promoted Cleavage of Triazolebearing Amine Derivatives and Its Application in the Detection of Ionic Gold. Chem. Commun. 2014, 50, 12352-12355.

Wang, E.; Pang, L.; Zhou, Y.; Zhang, J.; Yu, F.; Qiao, H.; Pang, X. A High Performance Schiff-base Fluorescent Probe for Monitoring Au3+ in Zebrafish Based on BODIPY. Biosens. Bioelectron., 2016, Vol.77, 812–817.

Ucuncu, M.; Karakus, E.; Emrullahoglu, M. A Ratiometric Fluorescent Probe for Gold and Mercury Ions. Chem. Eur. J. 2015, 21, 13201 – 13205.

Adhikari, S.; Mandal, S.; Ghosh, A.; Das, P.; Das, D. Strategically Modified Rhodamine − Quinoline Conjugate as a CHEF Assisted FRET Probe for Au3+: DFT and Living Cell Imaging Studies. J. Org. Chem. 2015, 80, 8530−8538.

Karakus, E.; Akdogan, G. C.; Emrullahoglu, M. A guanidinium Modified Rhodamine-Based Fluorescent Probe for in Vitro/Vivo Imaging of Gold Ions. Anal. Methods 2015, 7, 8004–8008.

Chinapang, P.; Ruangpornvisuti, V.; Sukwattanasinitt, M.; Rashatasakhon, P. Ferrocenyl Derivative of 1,8-naphthalimide as a New Turn-on Fluorescent Sensor for Au(III) Ion. Dyes and Pigments 2015, 112, 236-238.

APPENDIX A

^{1}H-NMR AND ^{13}C-NMR SPECTRA OF COMPOUNDS

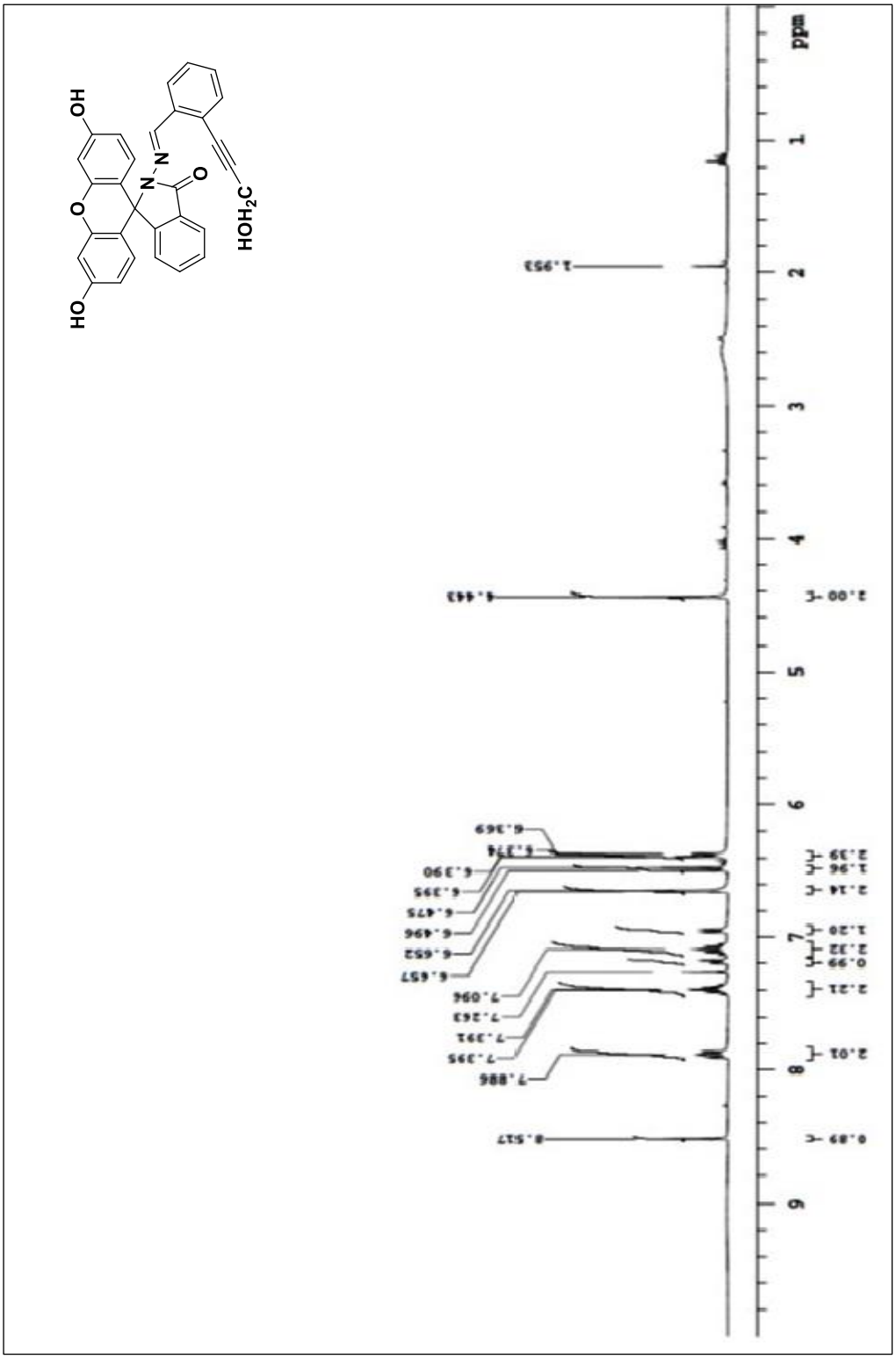

Figure A.1. ^{1}H NMR of **(probe-1)** 3',6'-dihydroxy-2-((2-(3-hydroxyprop-1-yn-1yl)benzylidene) amino)spiro[isoindo line-1,9'-xanthen]-3-one

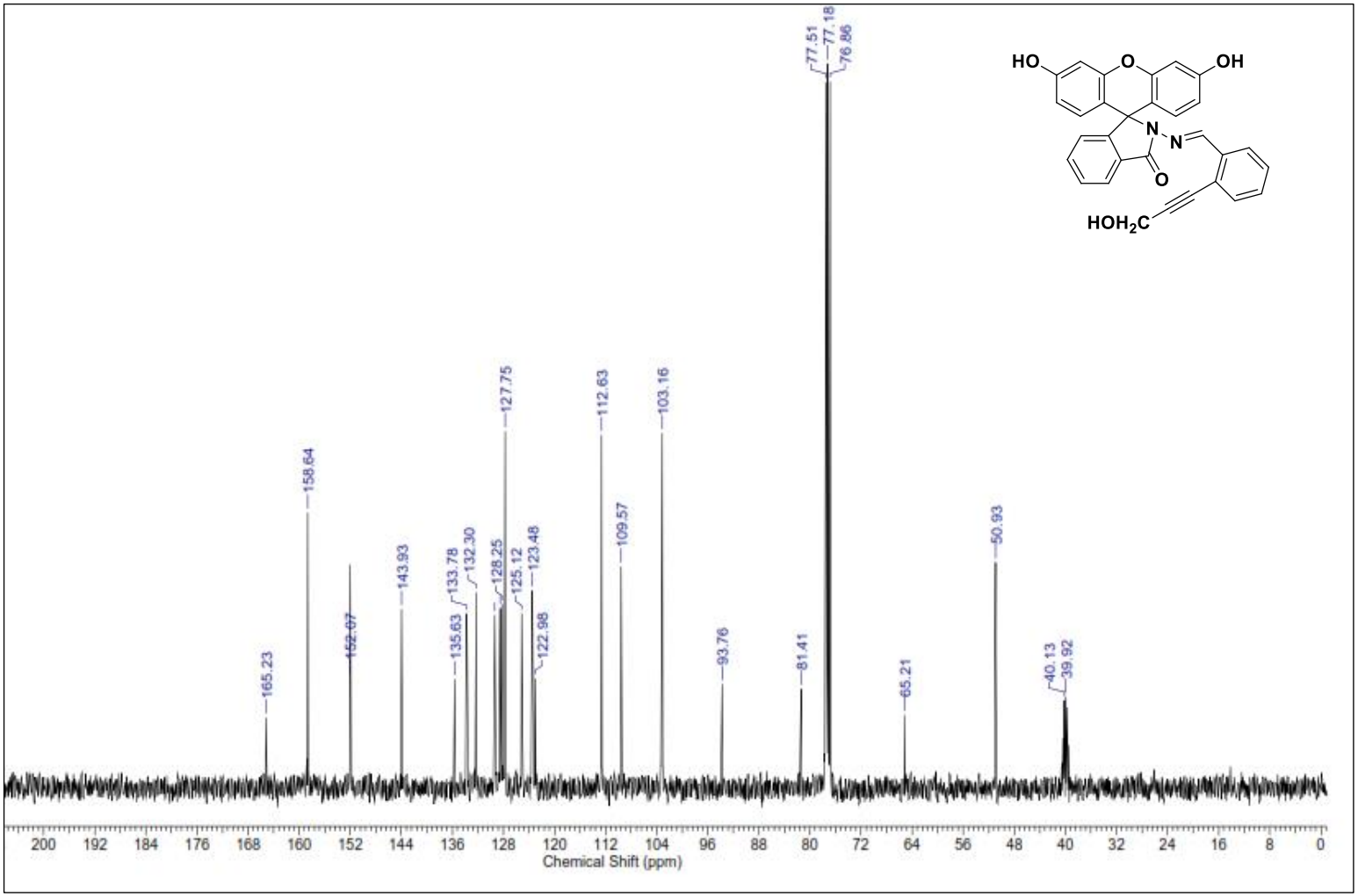

Figure A.2. ^{13}C NMR of **(probe-1)** 3',6'-dihydroxy-2-((2-(3-hydroxyprop-1-yn-1-yl)benzylidene) amino)spiro [isoindo line-1,9'-xanthen]-3-one

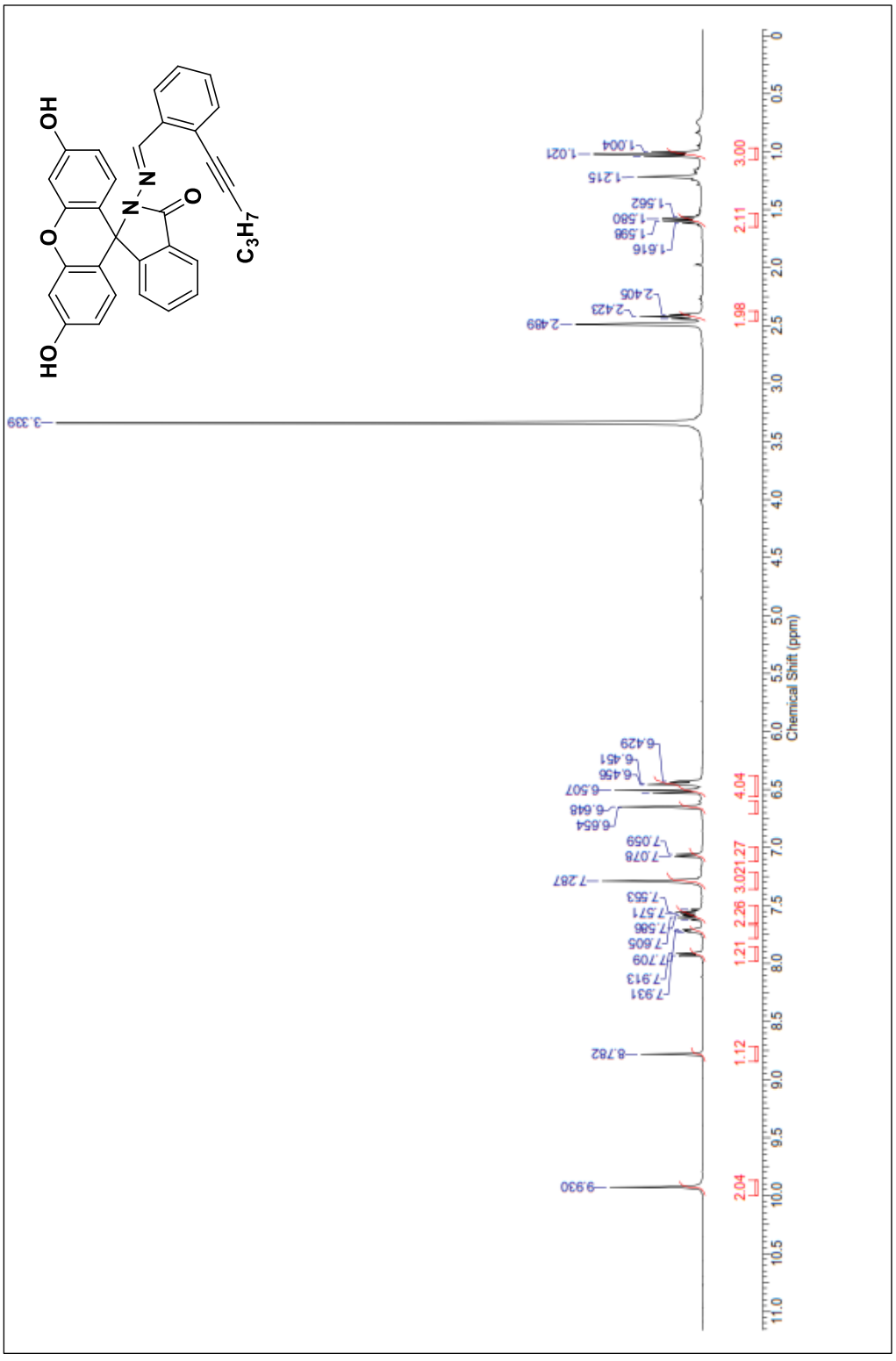

Figure A.3. ^{1}H NMR of **(probe-2)** 3',6'-dihydroxy-2-((2-(pent-1-yn-1yl)benzylidene)amino) spiro[i soindoline-1,9'-xanthen]-3-one

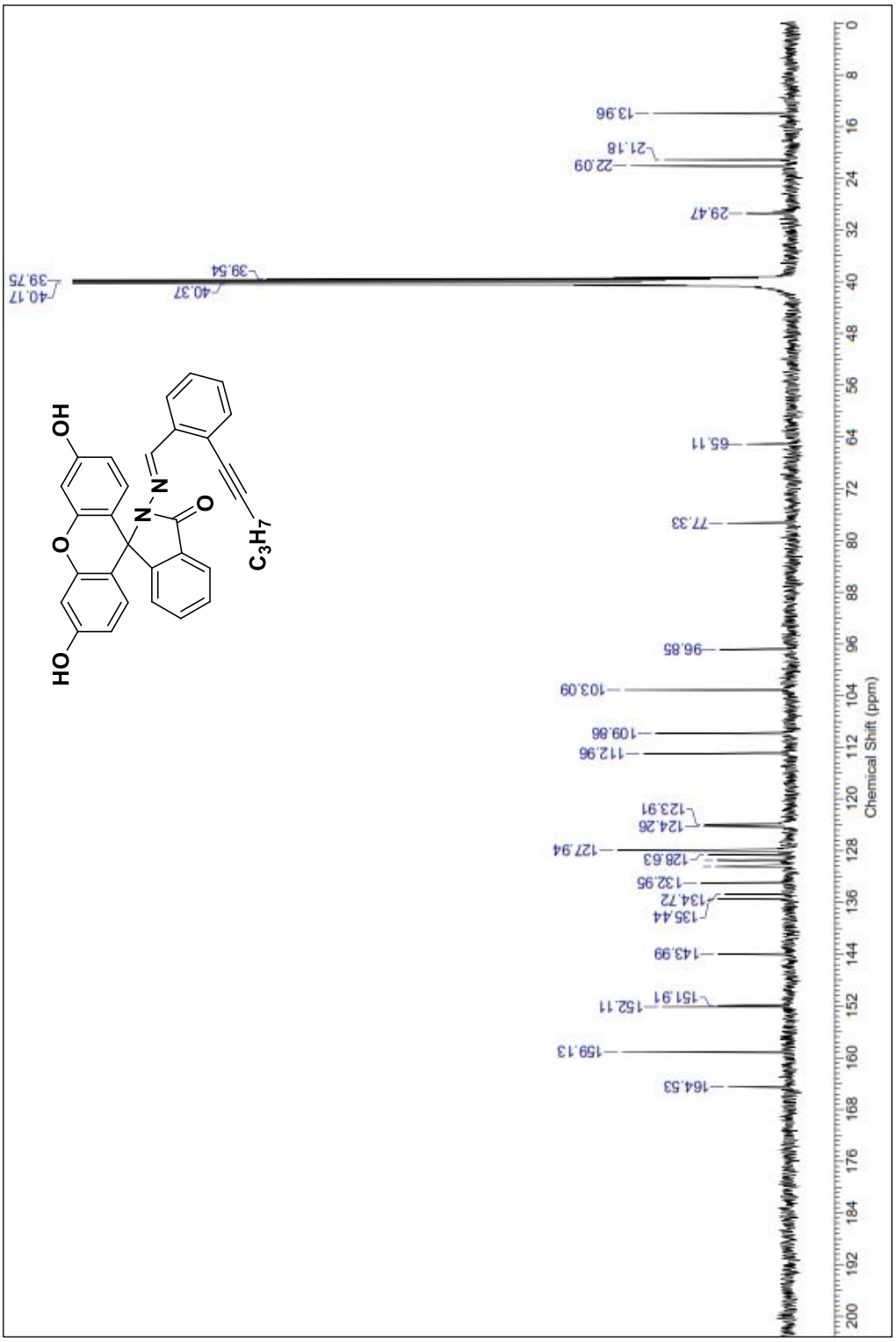

Figure A.4. ^{13}C NMR of **(probe-2)** 3',6'-dihydroxy-2-((2-(pent-1-yn-1yl)benzylidene)amino) spiro[i soindoline-1,9'-xanthen]-3-one

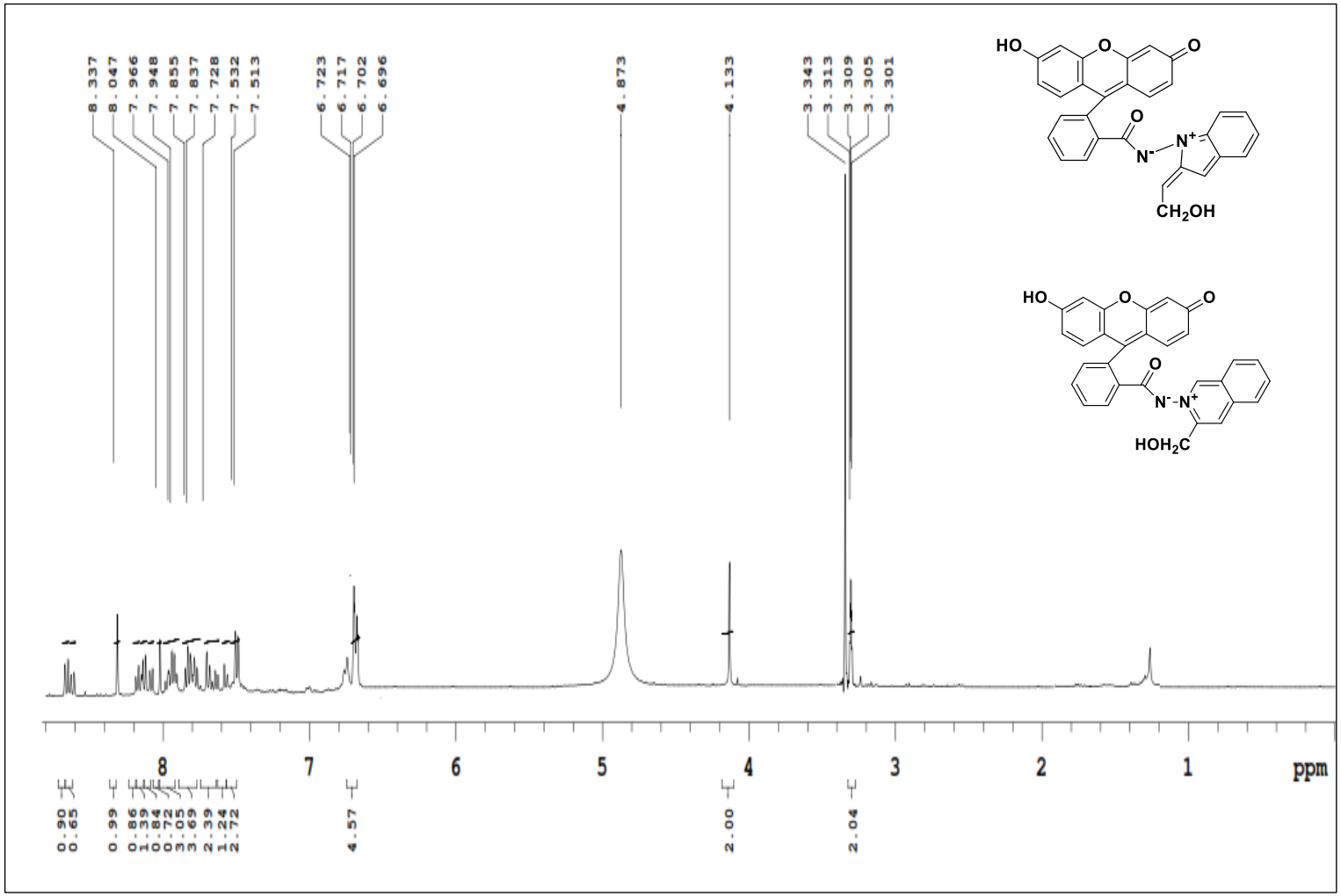

Figure A.5. ^{1}H NMR of **(probe-1P)** (2-(6-hydroxy-3-oxo-3H-xanthen-9-yl)benzoyl)(3-(hydroxymethyl)isoquinolin-2-ium-2-yl)amide and (E)-(2-(6-hydroxy-3-oxo-3H-xanthen-9-yl)benzoyl)(2-(2-hydroxyethylidene)-2H-indol-1-ium-1-yl)amide

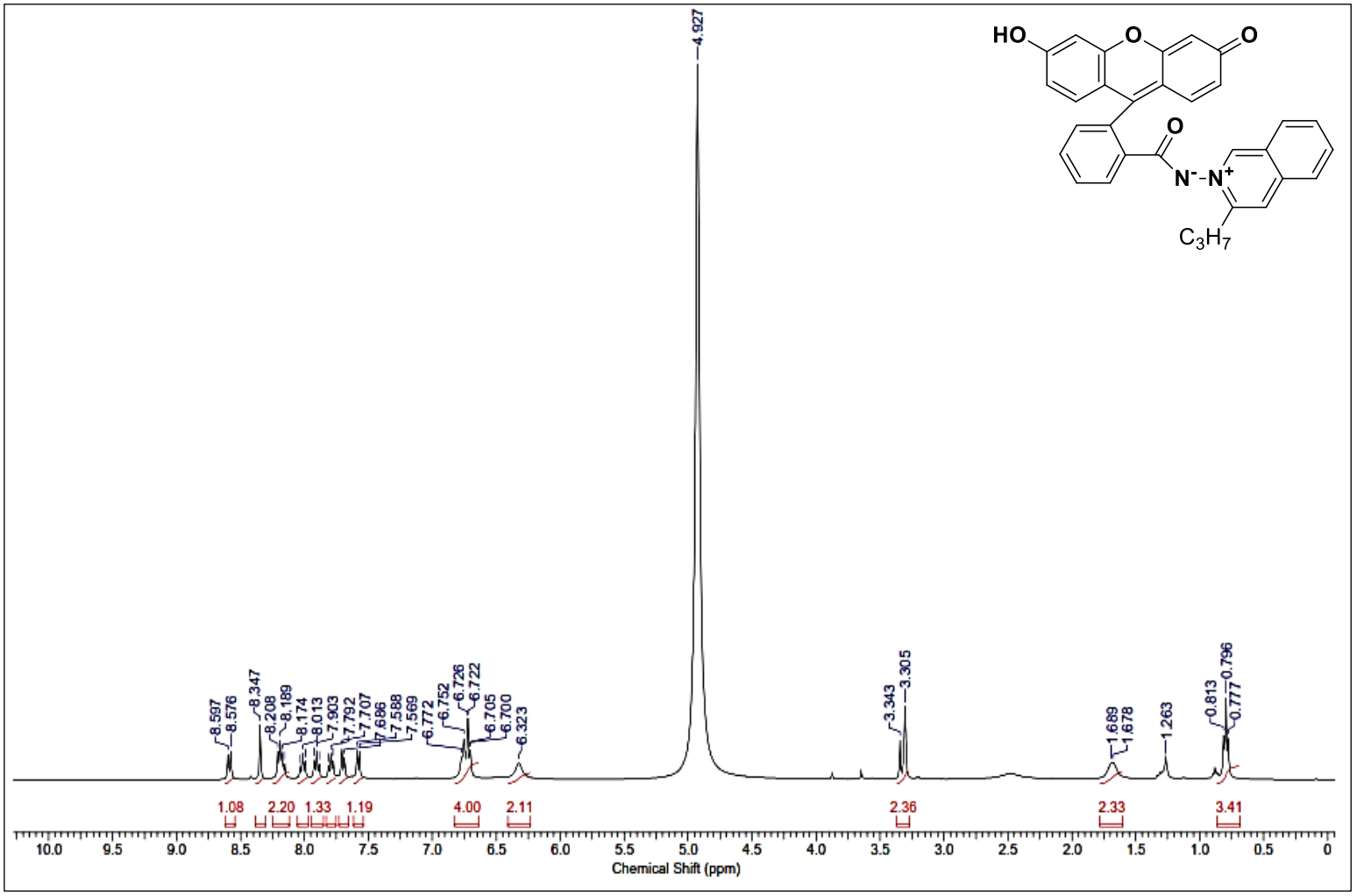

Figure A.6. ^{1}H NMR of **(probe-2P)** (2-(6-hydroxy-3-oxo-3H-xanthen-9-yl)benzoyl)(3-propylisoquinolin 2-ium-2-yl)amide

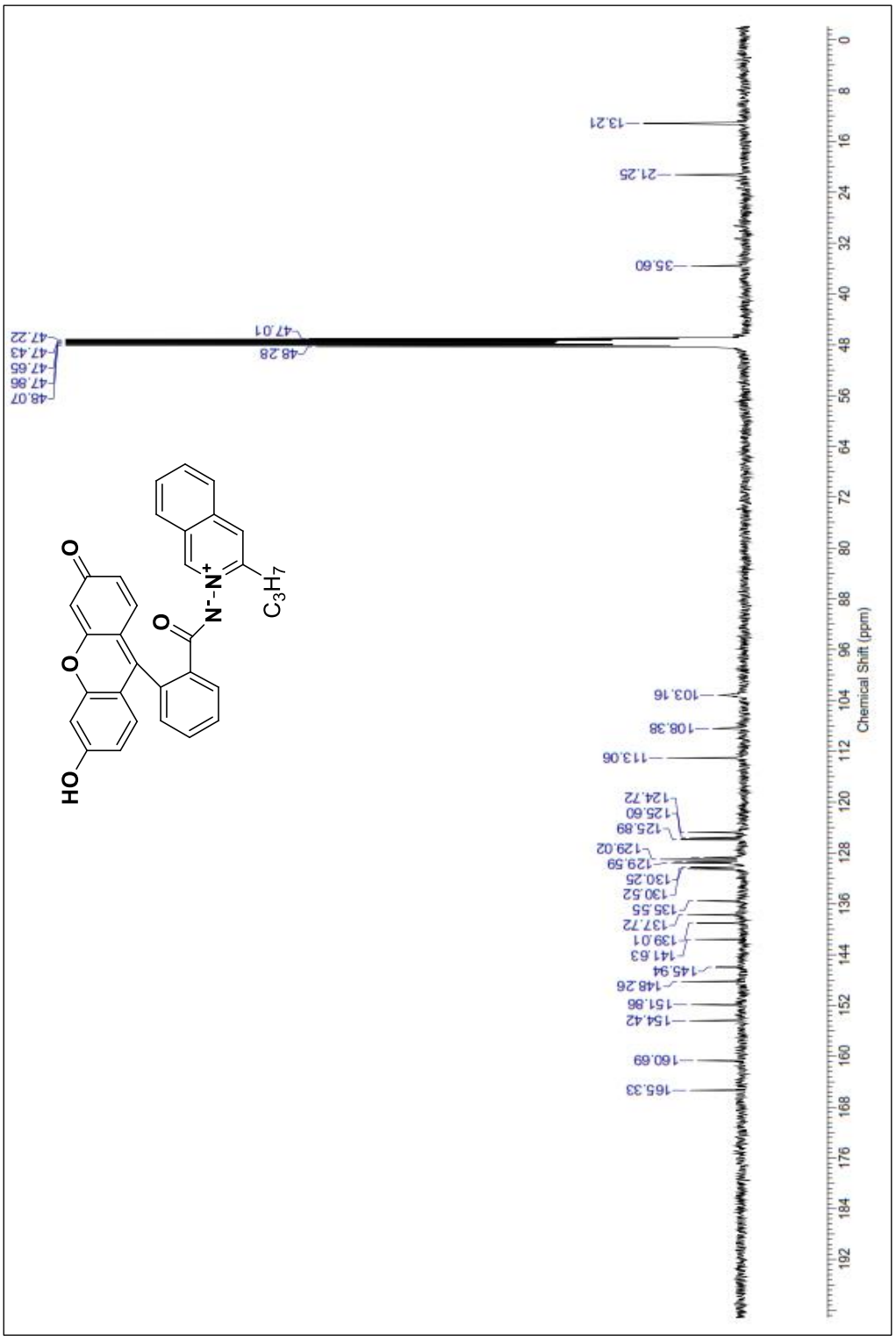

Figure A.7. ^{13}C NMR of **(probe-2P)** (2-(6-hydroxy-3-oxo-3H-xanthen-9-yl)benzoyl)(3-propylisoquinolin 2-ium-2-yl)amide

APPENDIX B

MASS SPECTRA OF COMPOUNDS

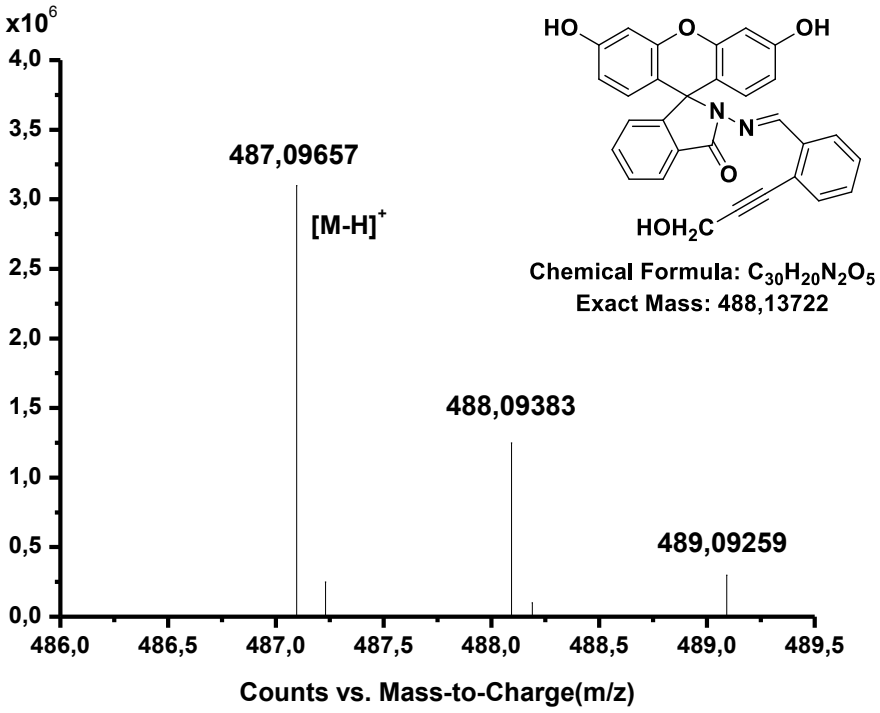

Figure B.1. Mass Spectrum of **probe-1** 3',6'-dihydroxy-2-((2-(3-hydroxyprop-1-yn-1-yl)benzylidene) amino)spiro [isoindo line-1,9'-xanthen]-3-one

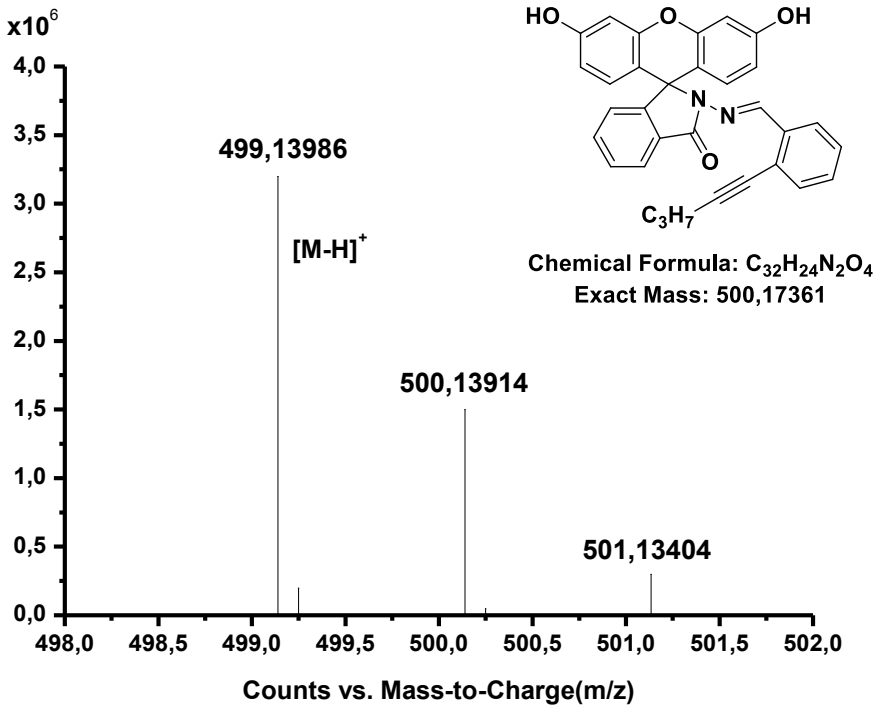

Figure B.2. Mass Spectrum of **probe-2** 3',6'-dihydroxy-2-((2-(pent-1-yn 1yl)benzyl idene)amino)spiro[isoindoline-1,9'-xanthen]-3-one

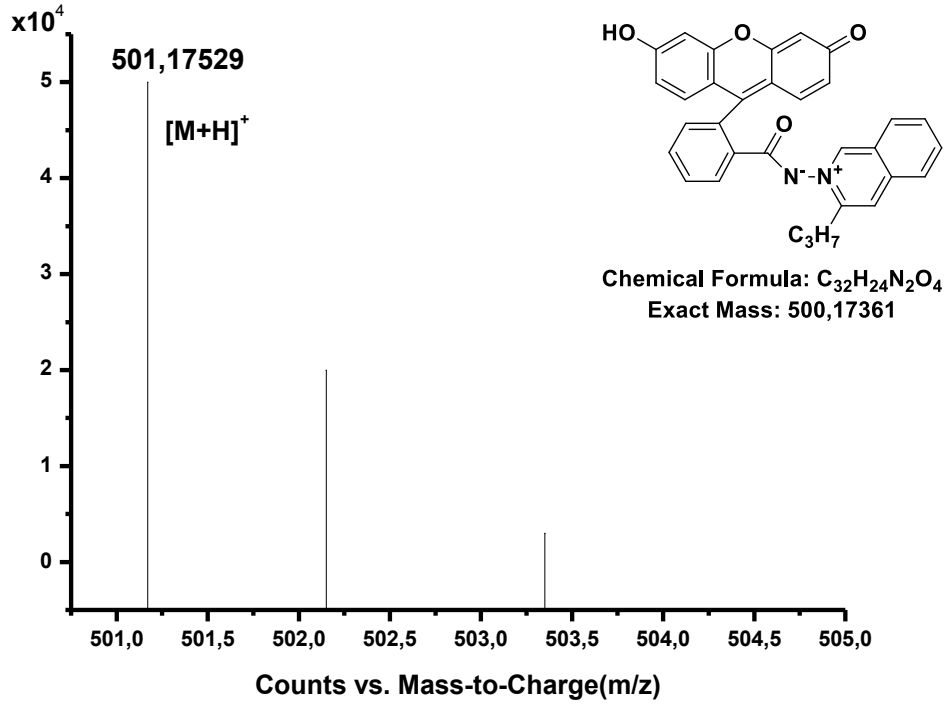

Figure B.3. Mass Spectrum of **probe-2P** (2-(6-hydroxy-3-oxo-3H-xanthen-9-yl)benzoyl) (3-propylisoquinolin-2-ium-2-yl)amide